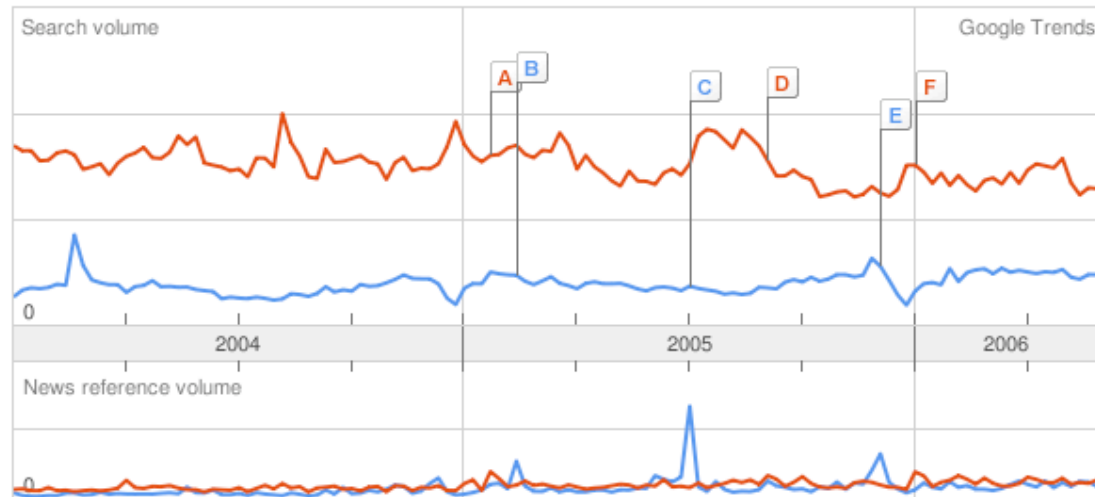


A review of **Hurricane Variability**

Balu Nadiga, COSIM, LANL, Jun 2006

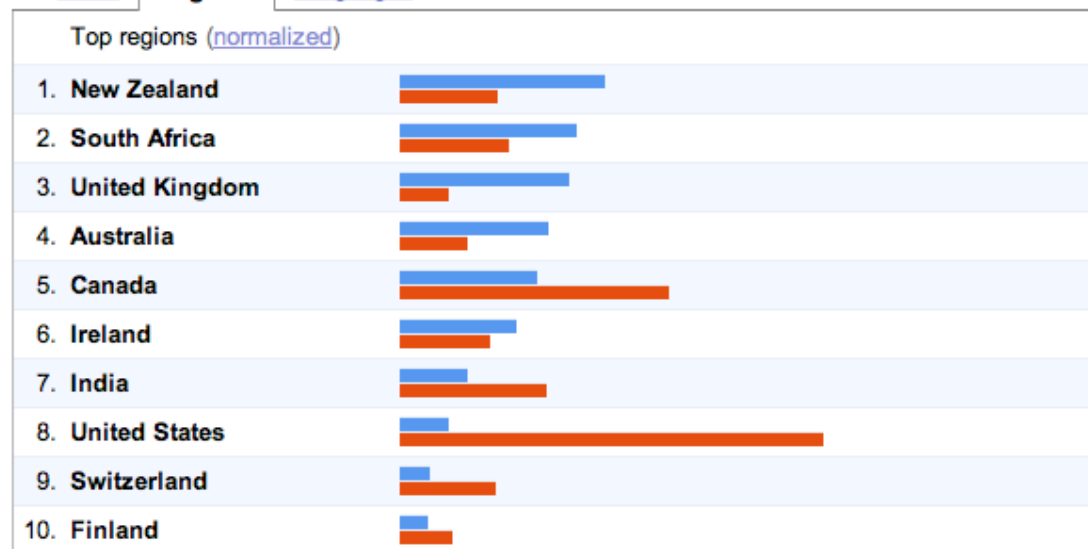
NASA

● climate change ● suv



- A [10 Die, 180 Hurt After Train Hits SUV](#)
Guardian Unlimited - Jan 27 2005
- B [Climate Change](#)
Politics.co.uk - Feb 16 2005
- C [G8 and climate change](#)
Politics.co.uk - Jul 7 2005
- D [Toyota recalling nearly 1 million SUV's and pickup trucks](#)
WKYC-TV - Sep 7 2005
- E [Climate Change Conference Leaves US Behind](#)
The New Mexico Channel.com - Dec 10 2005
- F [Cat Rides 70 Miles Under SUV](#)
NBC6.net - Jan 5 2006

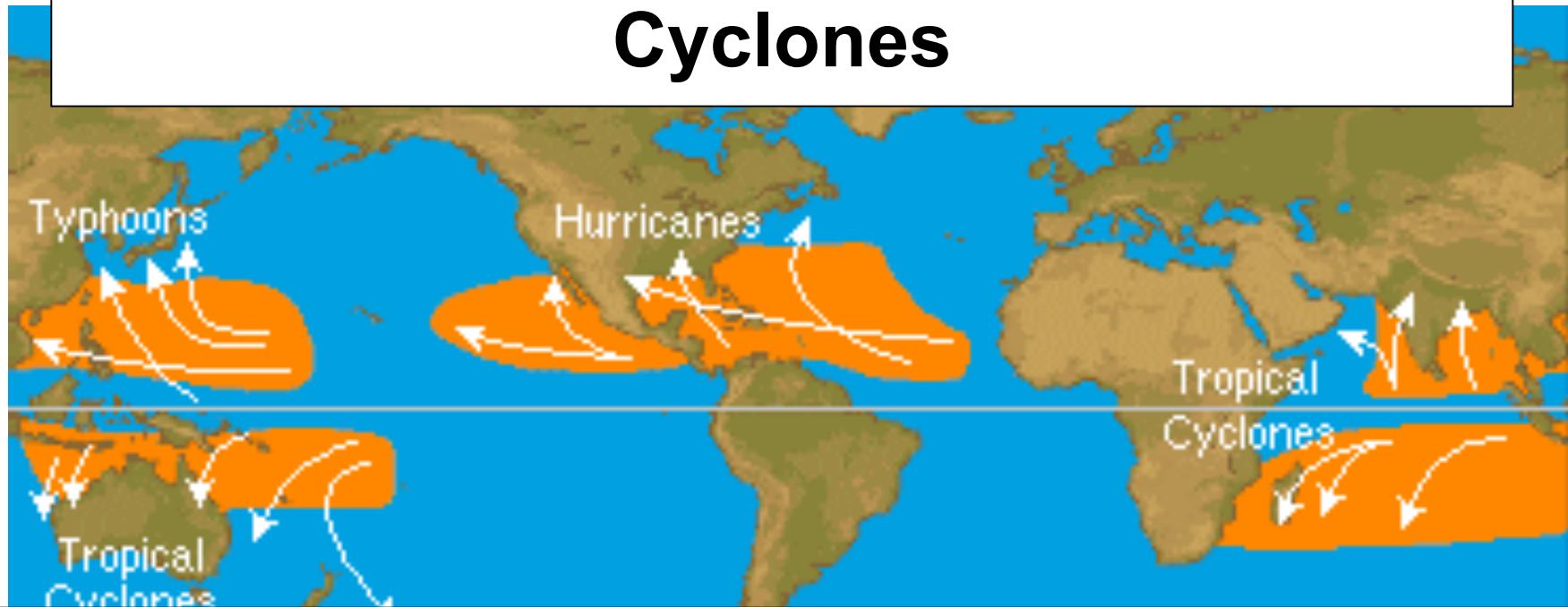
Cities **Regions** Languages



Key Sources

- Kerry Emanuel
- Webster 2005
- Elsner 1996
- NASA, NOAA, NCAR
- Others

Hurricanes, Typhoons, Tropical Cyclones



- Tropical Oceanic Weather System (SST > 26 C)
- Max. Sustained Winds > 74mph
- About 500 km diameter (so, rotation important)
- Smaller than mid-latitude storm systems
- Seldom equatorward of 5 Lat (because rotation important)

Hurricanes: A few Comments

- Acts as a heat engine, but with crucial fluid dynamic controls
- Ocean atmosphere interactions not fully understood
- Hurricanes are extreme events
- Coherent structures, Intermittency of Turbulence
- In that sense, statistics of hurricanes are related to higher order statistics as opposed to say global mean temperatures or mean circulation which are of low order
- However, hurricanes are fuelled by upper ocean heat which itself is a low order quantity
- Deterministic Chaos—Initial small errors leading to exponential divergence of trajectories. Limit of deterministic predictability render purely dynamical forecasts insufficient for particular hurricanes, but what about for statistics?

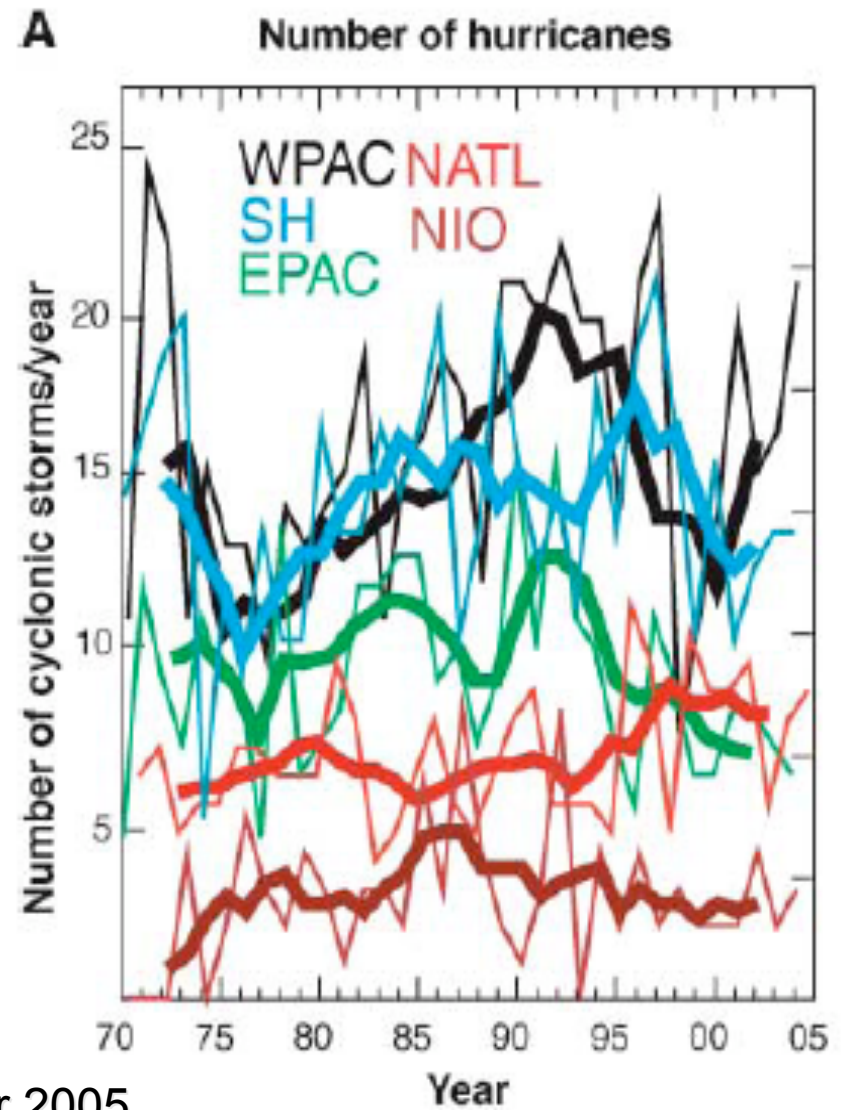
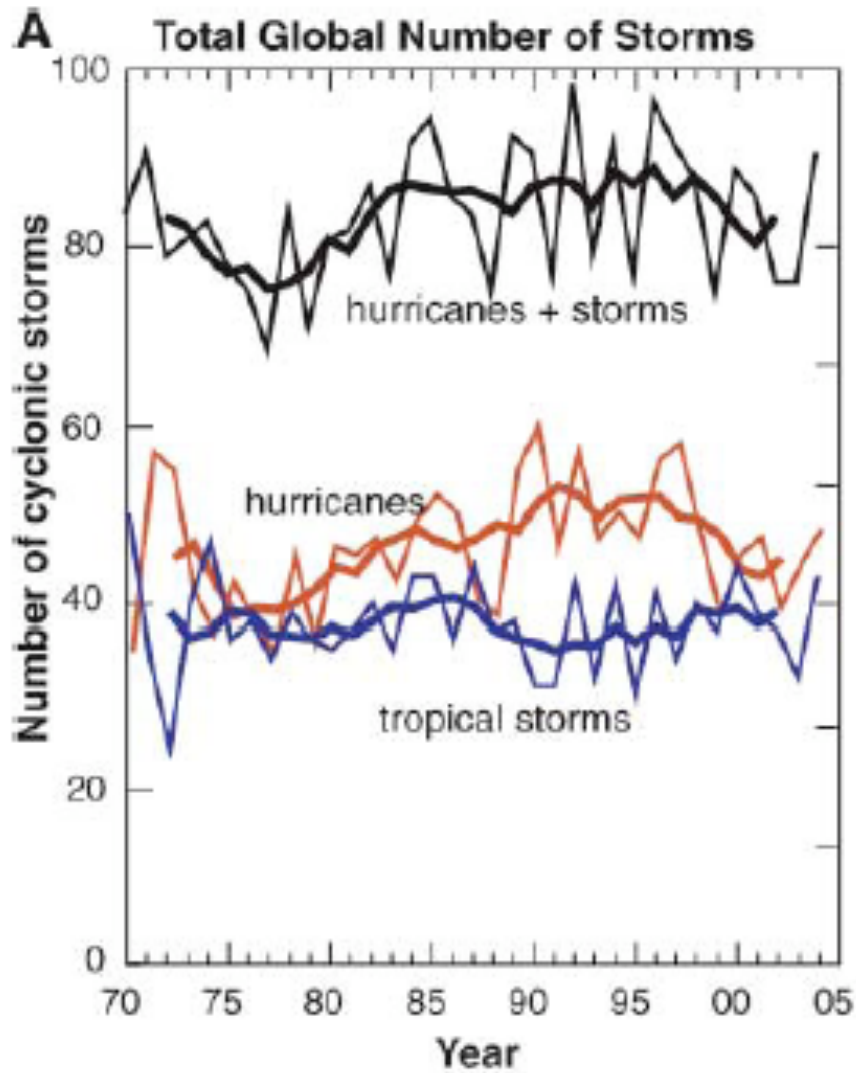
Is global warming causing a change in hurricane variability?

Difficult question to answer because

- No detectable trend in historical annual frequency data either globally or regionally. **But there seems to be a trend in the SST in the formation regions!**
- Note, however, that interannual variability of frequency can be large, particularly in individual basins. Almost understandably, interannual variability in global frequency is smaller.
- Possible influence of ENSO, QBO, NAO, AMO, ...
- Global climate model predictions of storm frequency are highly inconsistent. But, most simulations predict an increase in intensity (may be too early to clearly see effects on intensity?)

JIST: SST in source regions shows trend, but not frequency. So, is intensity being modified?

No statistically significant trend in either global or regional frequency



Webster 2005

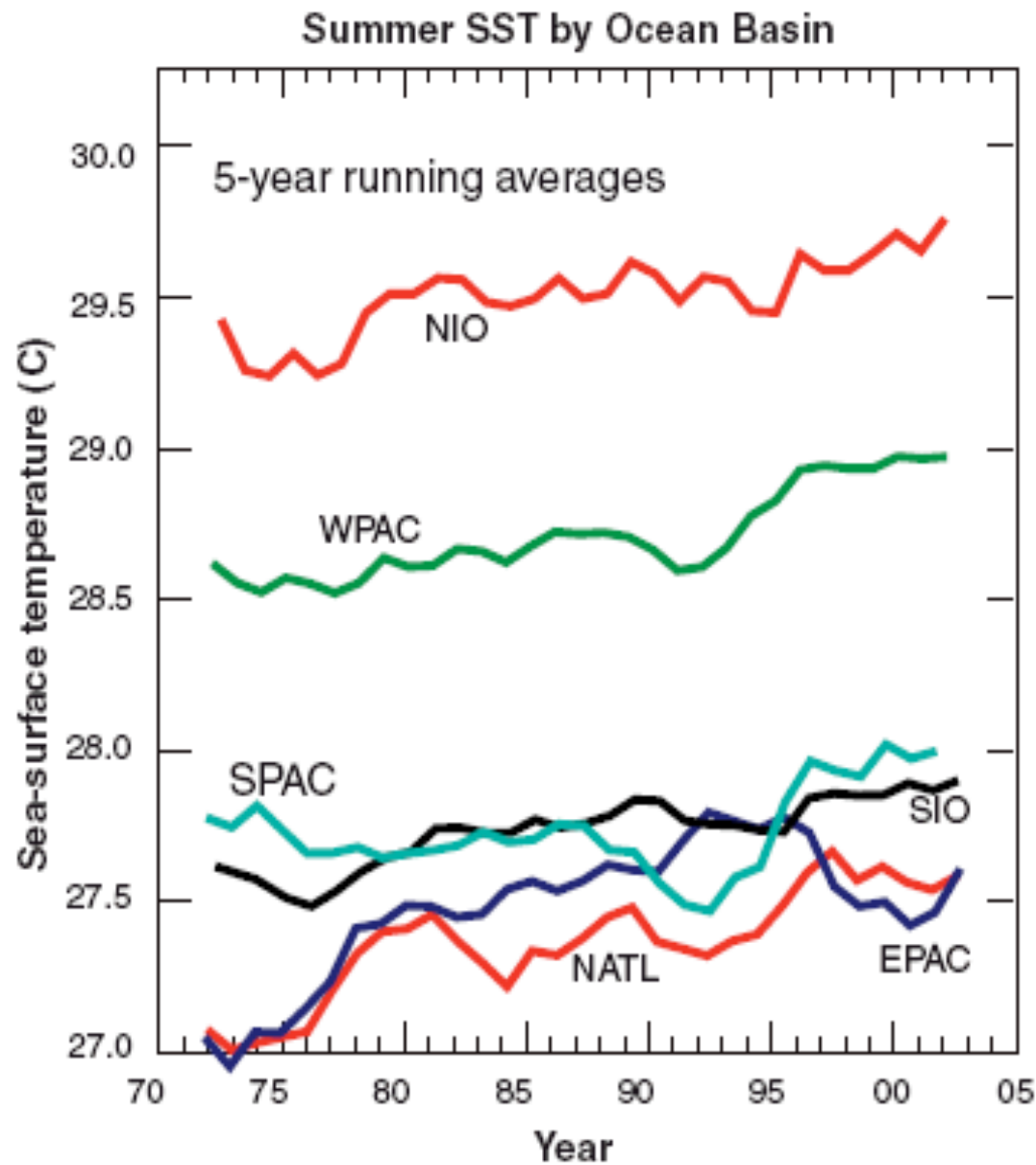


Fig. 1. Running 5-year mean of SST during the respective hurricane seasons for the principal ocean basins in which hurricanes occur: the North Atlantic Ocean (NATL: 90° to 20°E, 5° to 25°N, June-October), the Western Pacific Ocean (WPAC: 120° to 180°E, 5° to 20°N, May-December), the East Pacific Ocean (EPAC: 90° to 120°W, 5° to 20°N, June-October), the Southwest Pacific Ocean (SPAC: 155° to 180°E, 5° to 20°S, December-April), the North Indian Ocean (NIO: 55° to 90°E, 5° to 20°N, April-May and September-November), and the South Indian Ocean (SIO: 50° to 115°E, 5° to 20°S, November-April).

Webster 2005

Why would SST affect intensity more than frequency

- Higher SST implies increased water vapor in lower troposphere (relative humidity remains approximately constant)
- Increased energy for tropical convection
- One aspect of intensified hydrological cycle due to global warming
- However, hurricanes are extreme events and their formation intricate with wind shear and other fluid dynamic processes exerting crucial control. Note, however, that this was an idea for a failed LDRD-ER
- But, the point is once there is a tropical disturbance/storm, there is a larger energy source to tap into

Strong Inter-annual, Inter-decadal Variability

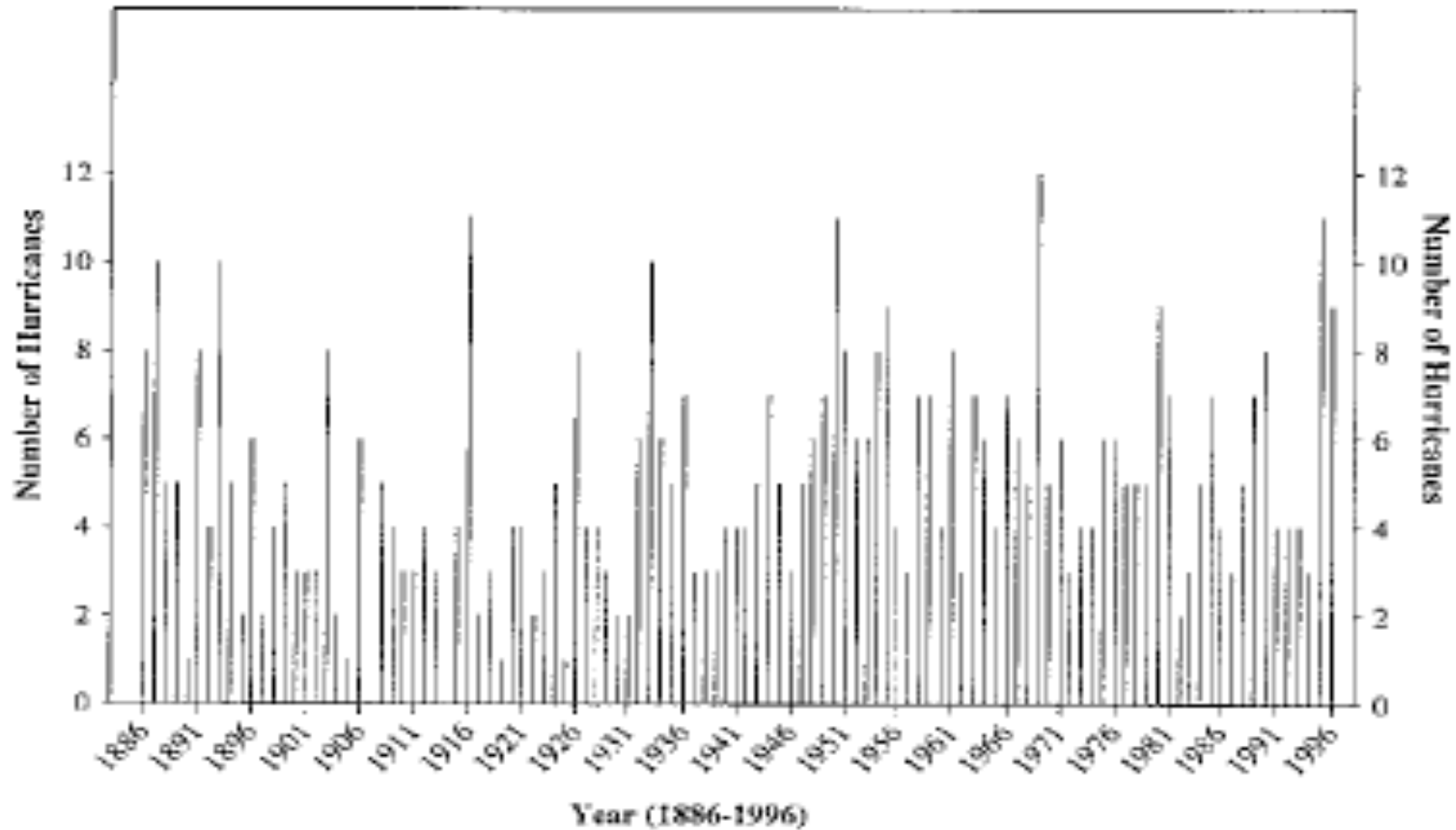
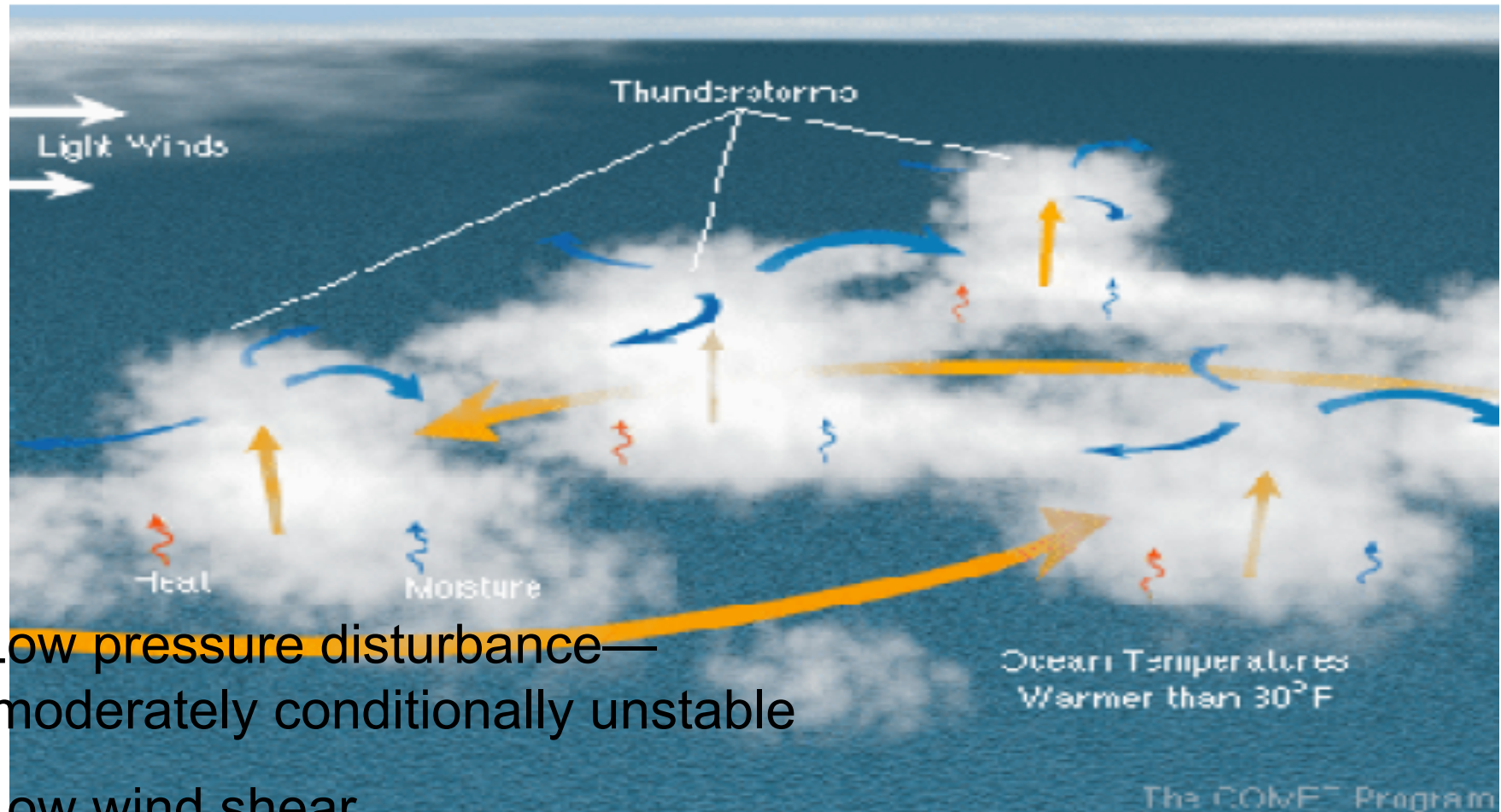


FIG. 1. Time series of the annual frequency of North Atlantic hurricanes over the period 1886–1996. The greatest number of hurricanes in a single season is 12 during 1969. Note the low frequency change in annual abundance over the 111-yr period.

(Elsner, 1996)

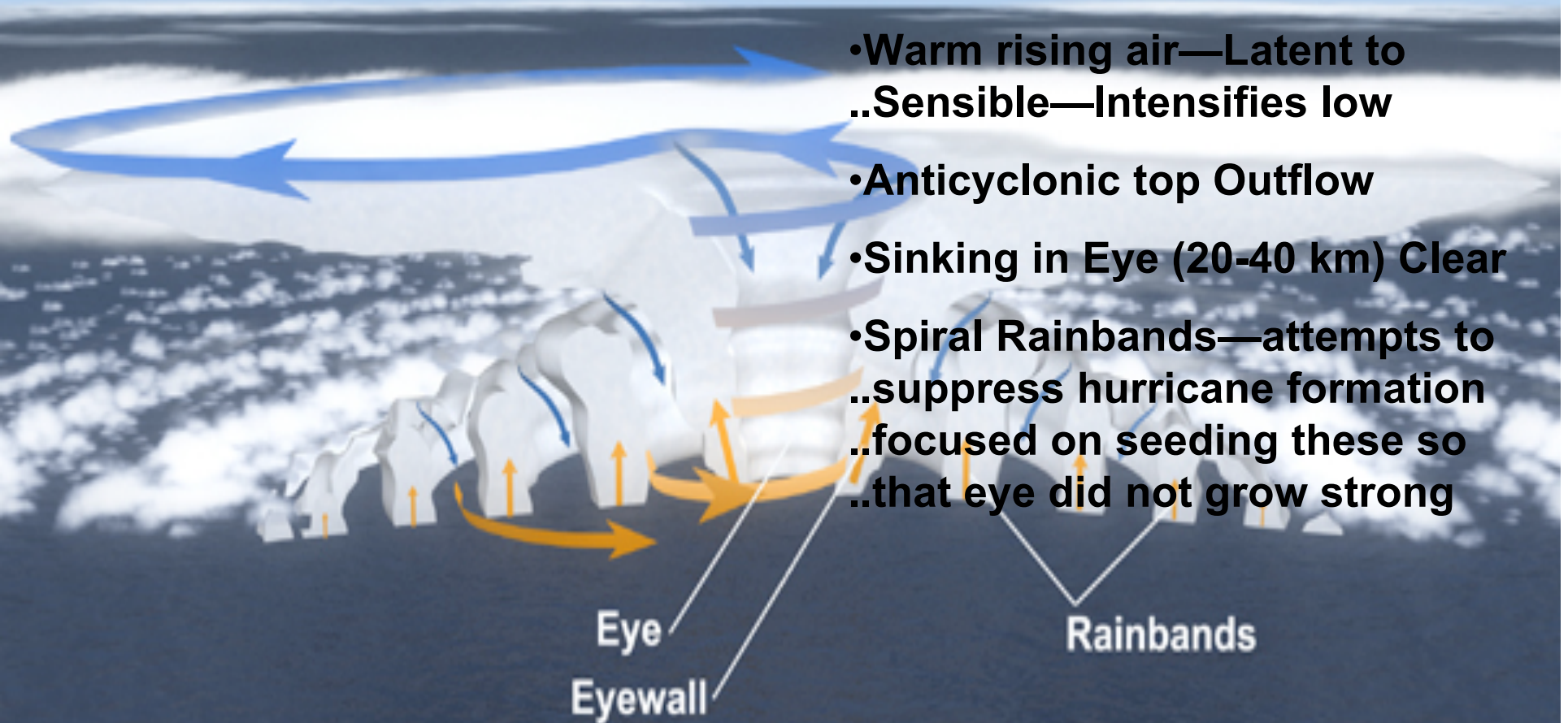
Necessary Conditions for Hurricane Formation



- Low pressure disturbance—
..moderately conditionally unstable
- Low wind shear
- SST > 26 C

Structure of an Hurricane

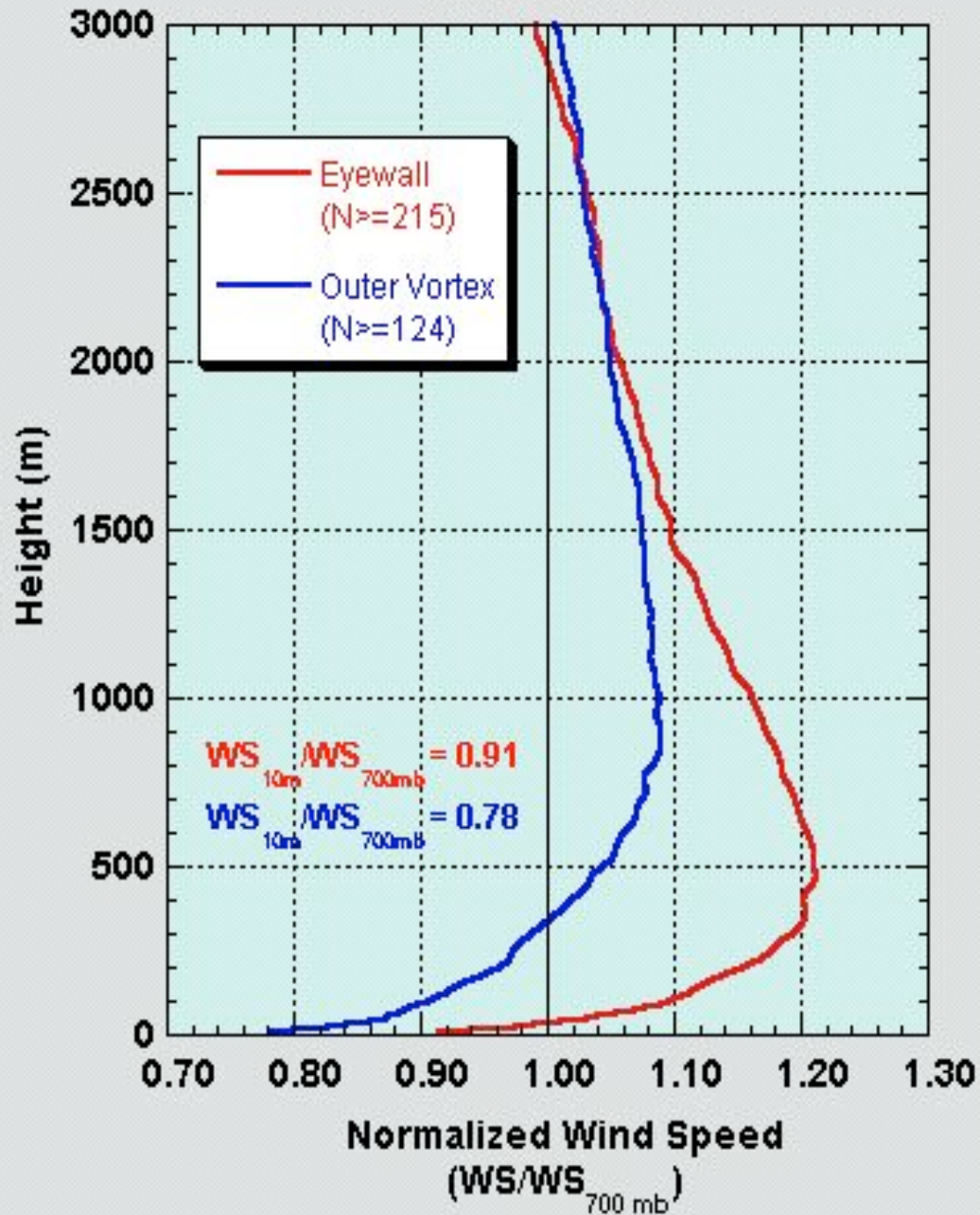
- **Spiral Cyclonic Surface Inflow**—
 - .. Latent heat flux from ocean
- **Warm rising air**—Latent to
 - .. **Sensible**—Intensifies low
- **Anticyclonic top Outflow**
- **Sinking in Eye (20-40 km) Clear**
- **Spiral Rainbands**—attempts to
 - .. suppress hurricane formation
 - .. focused on seeding these so
 - .. that eye did not grow strong



Hurricane Animation (NASA Scientific Visualization Studio)



Mean Wind Speed Profiles All Storms



Vertical Cross-section of winds

(<http://twister.ou.edu/MM2005/Chapter4.pdf>)

radial
wind

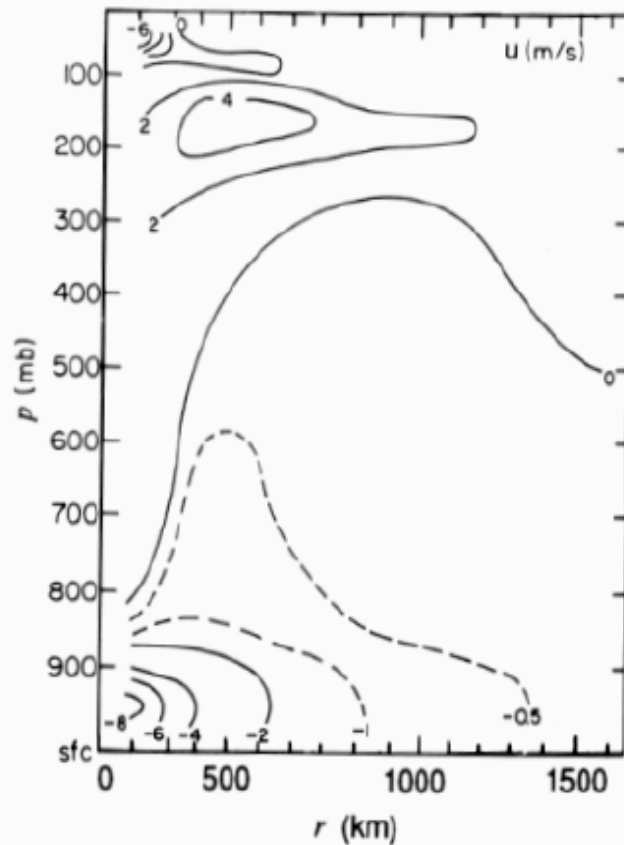


Figure 10.6

Figure 10.6 Vertical cross section of the mean radial wind (u) in western Atlantic hurricanes. Analysis is a composite of data collected in many storms. (From Gray, 1979. Reprinted with permission from the Royal Meteorological Society.)

tangential
wind

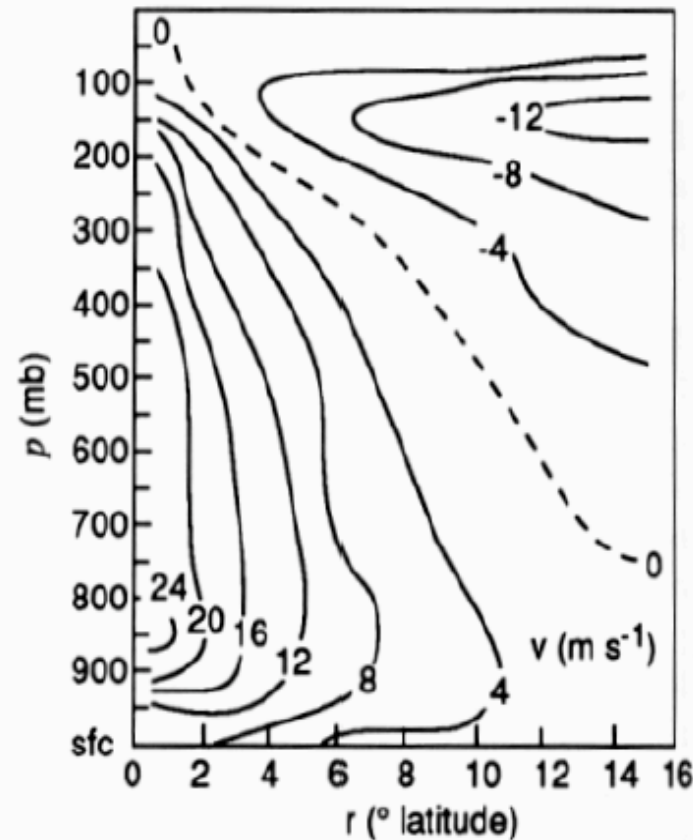
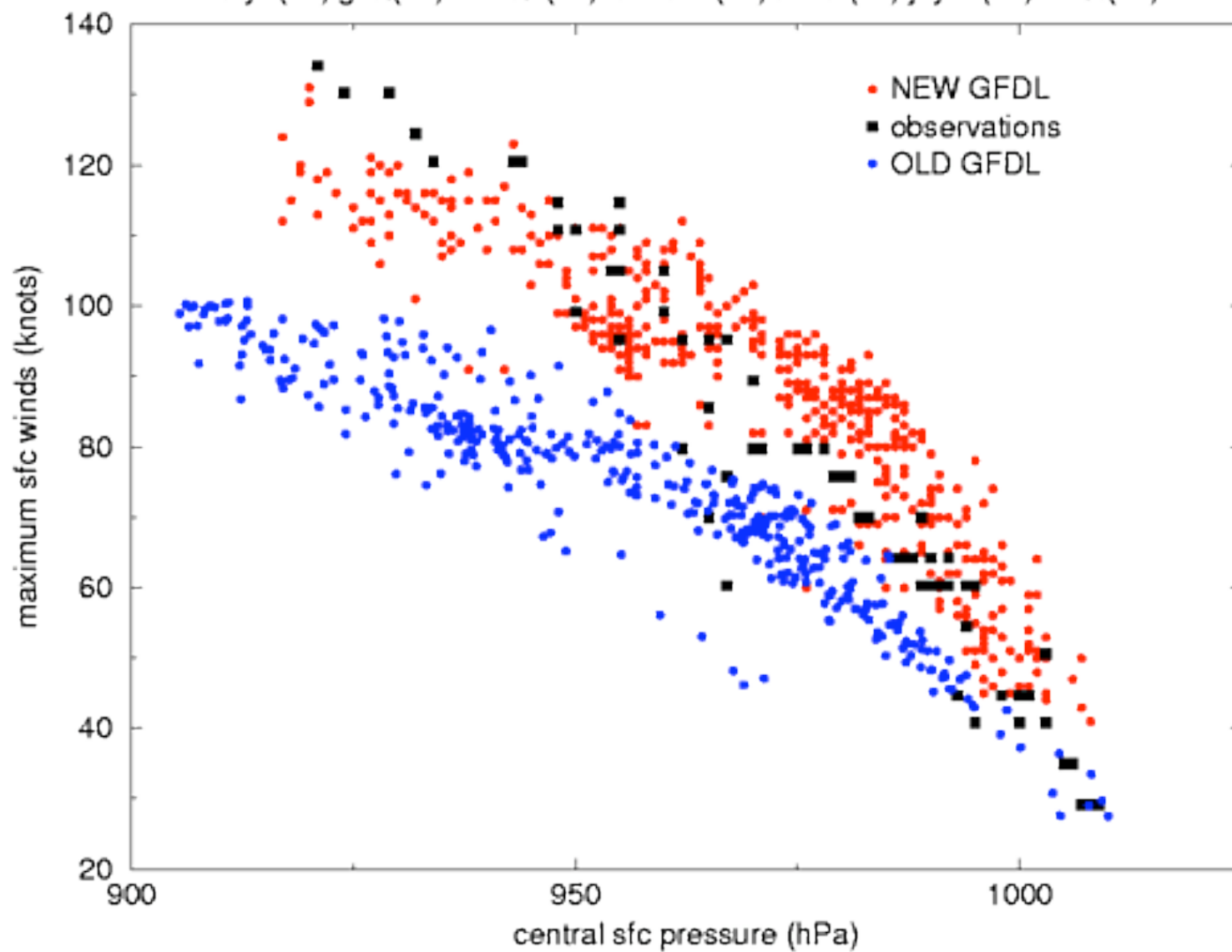


Figure 10.7

Figure 10.7 Vertical cross section of the mean tangential component of the wind (v) in Pacific typhoons. Analysis is a composite of data collected in many storms. (From Frank, 1977. Reprinted with permission from the American Meteorological Society.)

Wind-Pressure Relationship

floyd(99) gert(99) alberto(00) florence(00) isaac(00) joyce(00) keith(00)

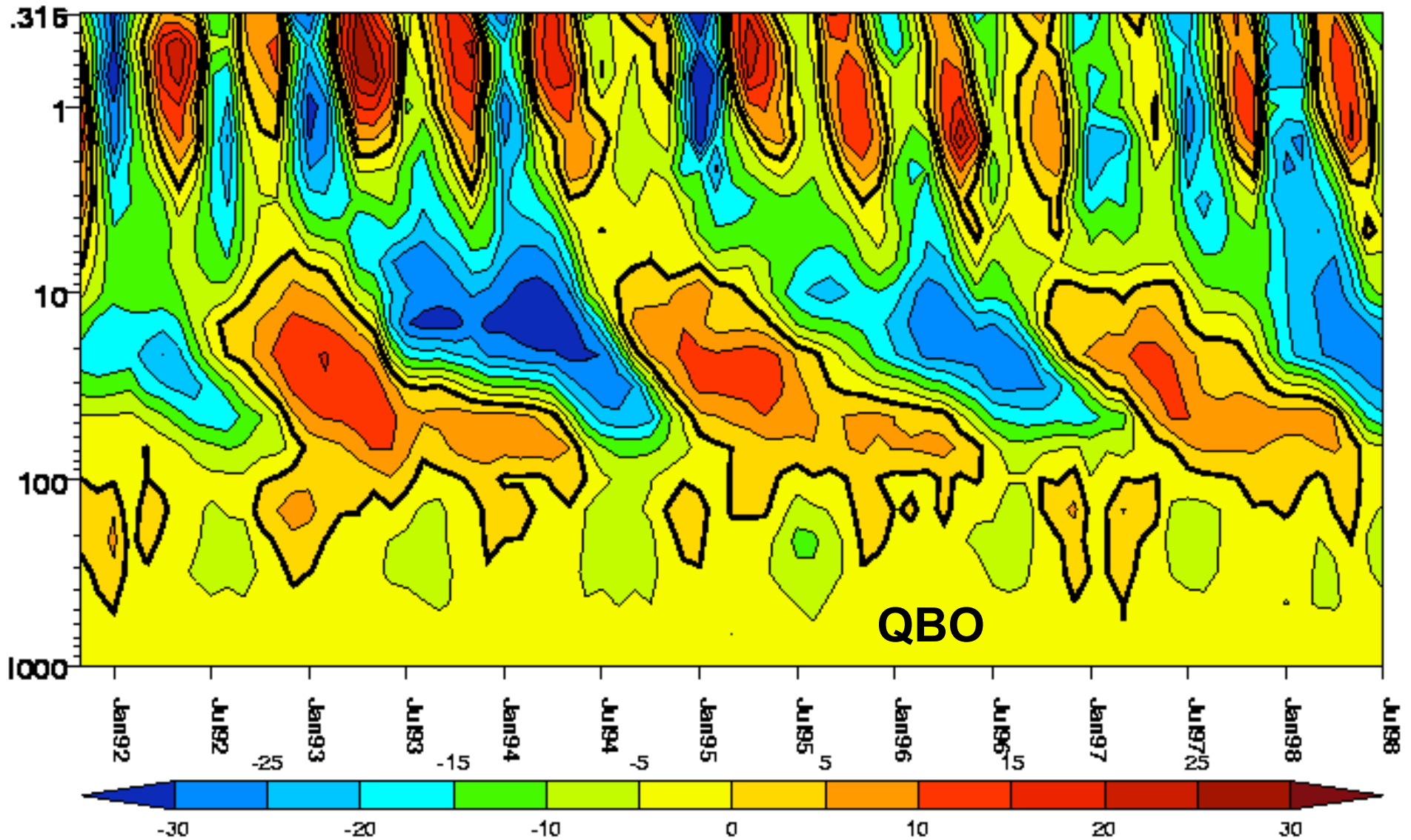


Saffir-Simpson Hurricane Intensity Scale

Category	Wind Speed (mph)	Storm Surge (m)
1	74-95	1-2
2	96-110	2-3
3	111-130	3-4
4	131-155	4-6
5	>155	>6

Analysis of Tropical Cyclone Variability

- Composite analysis or the method of superposed epochs: Identify various occurrences of a particular event over time from an independent dataset. Count the variables from the dependent data at those particular event times.
 - Independent datasets: SST, QBO, ENSO, solar activity.
 - Dependent data: Various aspects of hurricane activity (Elsner 1999)
- Rather surprisingly, composite analyses implicates ENSO and QBO in modulating hurricane frequency on the interannual and interdecadal timescales
- QBO—vertically propagating waves transfer momentum from troposphere to stratosphere. The phase of the QBO affects hurricanes in the Atlantic. Increased hurricane activity occurs for westerly (or positive) zonal wind anomalies; reduced hurricane activity for easterly or negative zonal wind anomalies
- Warm phase of ENSO (El Niño)—Enhanced Convection in Central/Eastern Pacific—West to East winds in upper troposphere across tropical Atlantic—Upper level convergence and sinking—suppresses hurricane development

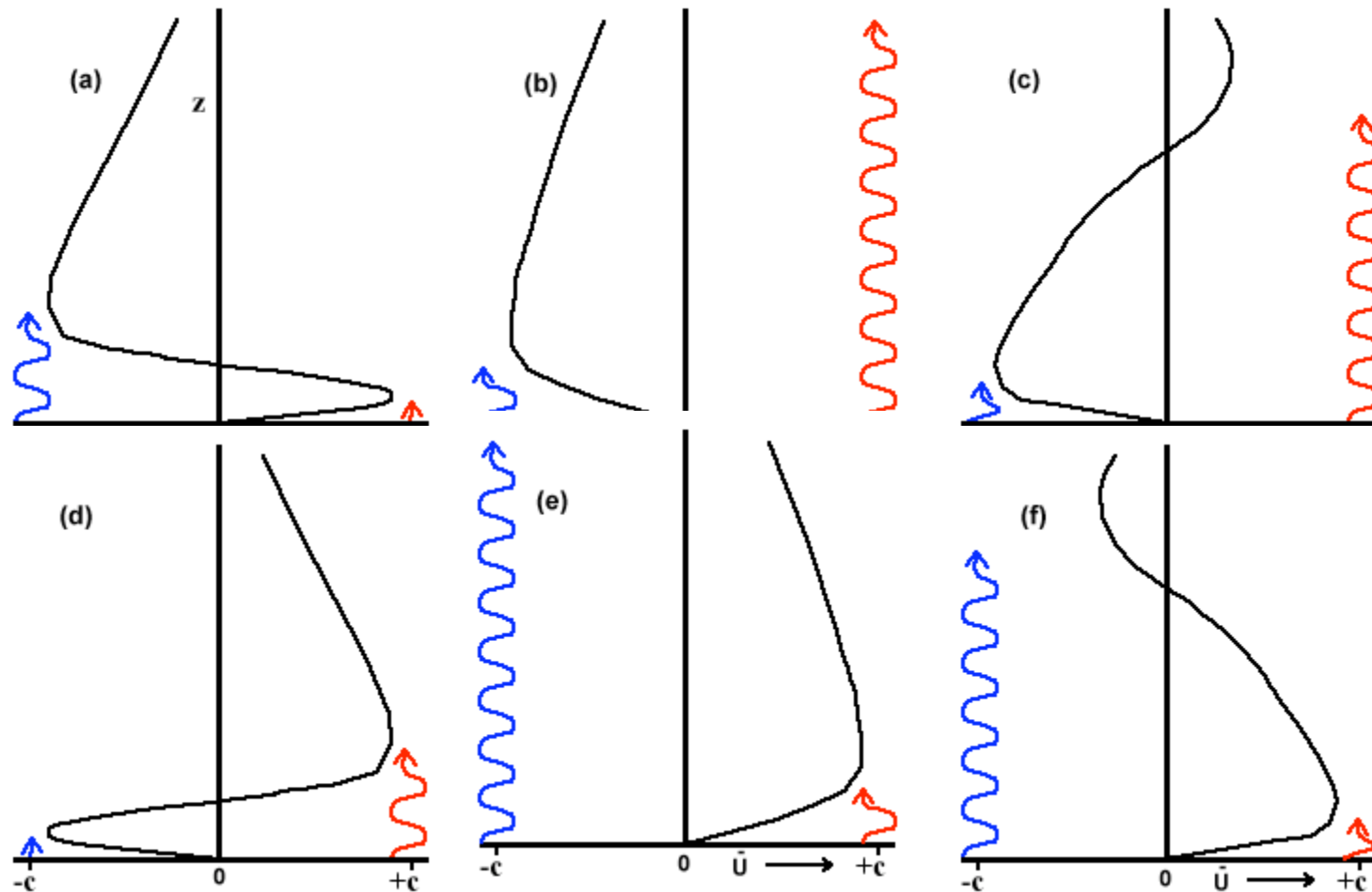


The monthly zonal mean wind in m/s against pressure in mb as seen in the UKMO assimilated dataset at 1.25° north of the equator. Easterlies are coloured yellow to blue and westerlies orange to red. The zero line is in thick black and every 5m/s is delineated in thin black. The QBO is roughly between 10mb and 100mb in height extent. Above 3mb the Semi-Annual Oscillation (SAO), a harmonic of the seasonal cycle can be seen, being westerly near the equinox and easterly near the solstice (<http://www.ugamp.nerc.ac.uk/hot/ajh/qbo.htm>)

Quasi Biennial Oscillation

(<http://www.ugamp.nerc.ac.uk/hot/ajh/qbo.htm>)

1. The wind regimes propagate down as time progresses.
2. They move downwards at roughly 1km/month and decrease in magnitude as the height decreases.
3. The period of the oscillation is 20 to 36 months with a mean of around 28 months.
4. They start at 10mb and descend to 100mb.
5. The maximum amplitude of 40 to 50m/s is seen at 20mb.
6. Easterlies are generally stronger than westerlies.
7. Westerly winds last longer than easterly winds at higher levels while the converse is true at lower levels.
8. The westerlies move down faster than the easterlies as shown by the steepness of the zero line.
9. The transition between westerly and easterly regimes is often delayed between 30 and 50mb.
10. There is considerable variability of the QBO in period and amplitude.



Plumb's analog of the QBO in six stages. Wavy blue: easterly Rossby-gravity waves; red: westerly equatorially trapped Kelvin waves. In **(a)** both easterly and westerly maxima are descending as the upward propagating waves deposit momentum just below the maxima. When the westerly shear zone is sufficiently narrow, viscous diffusion destroys the westerlies and the westerly waves can propagate to high levels through the easterly mean flow, **(b)**. The more freely propagating westerlies are dissipated at higher altitudes and produce a westerly acceleration leading to a new westerly regime, **(c)**. **(d)** shows both regimes descending downwards until the easterly shear zone becomes vulnerable to penetration and the easterlies can then propagate to high altitudes, **(e)**, and so onto the formation of a new easterly regime in **(f)**.

Detrended by Removing First EOF; N=111 yrs; M=15 yrs

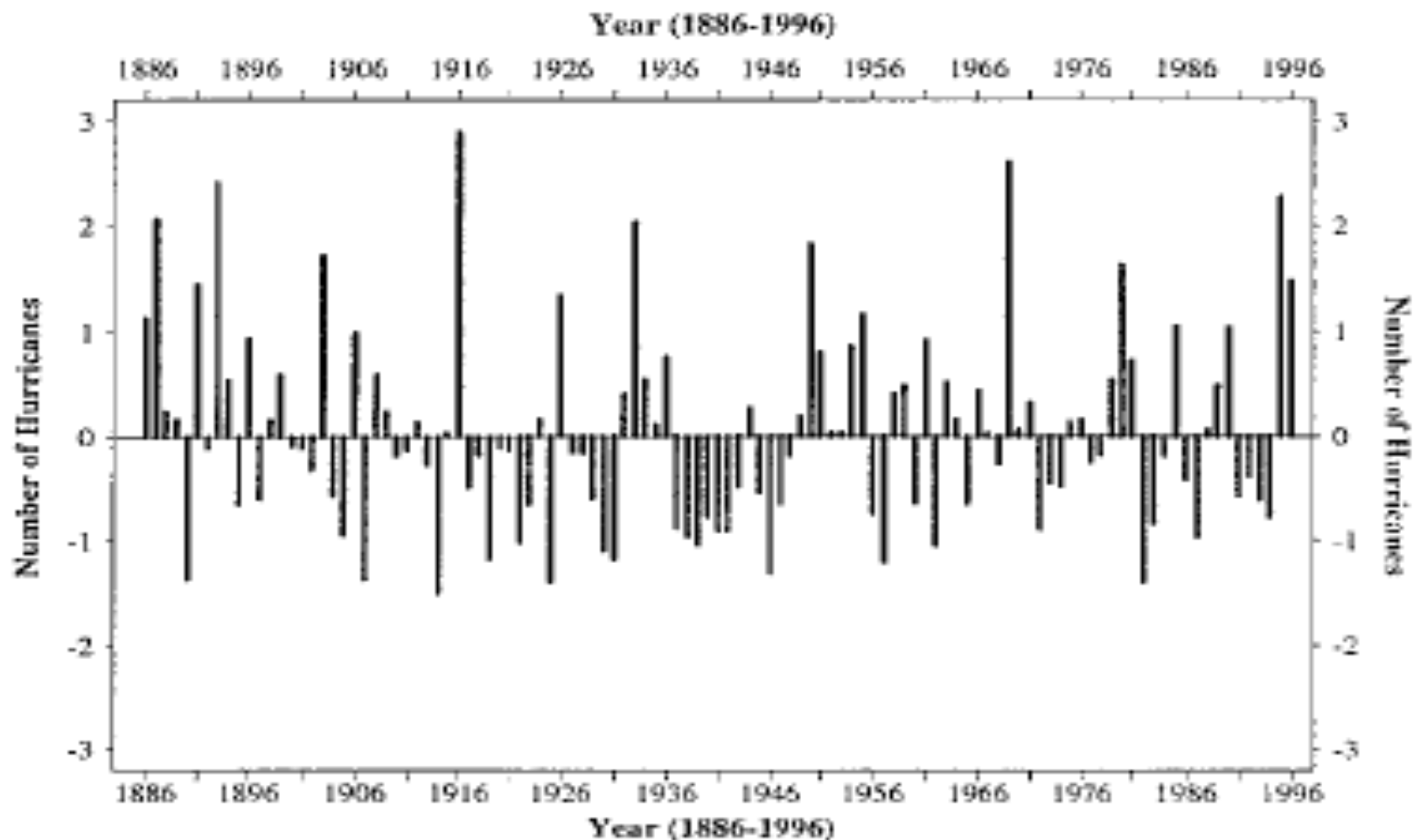


FIG. 2. Time series of annual North Atlantic basin hurricane frequencies over the period 1886–1996 after detrending by removing the leading ultra-low frequency temporal principal component.

SSA Reconstruction of 3 Leading Pairs (58% Variance Explained)

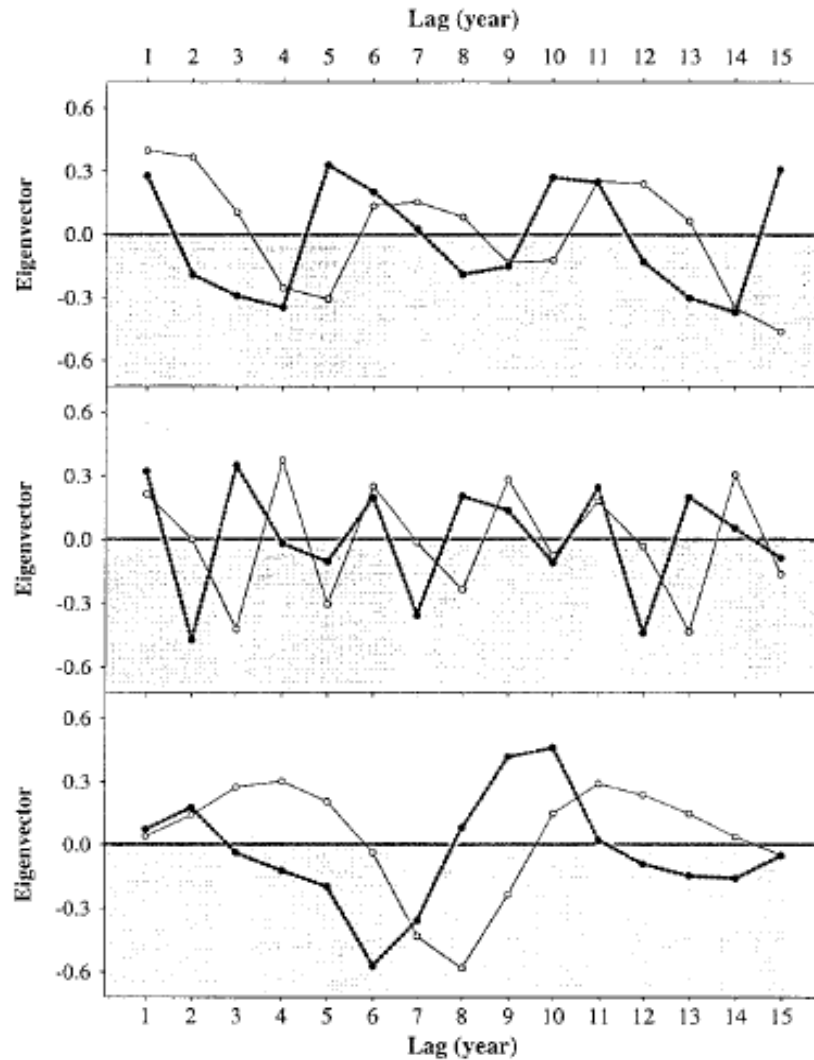


FIG. 4. Three leading eigenvector pairs of the detrended North Atlantic hurricane record. Each pair corresponds to a distinct oscillation in the annual hurricane record.

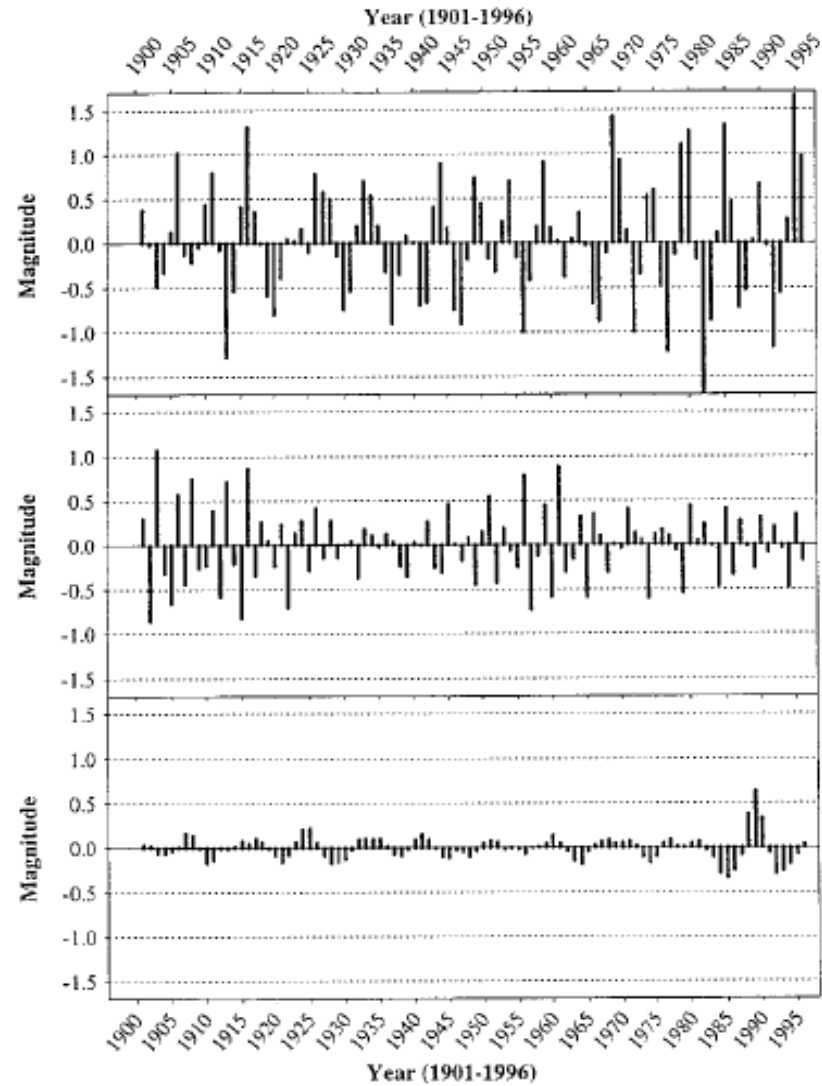


FIG. 5. Three dominant reconstructed components of the detrended North Atlantic hurricane record using the method of SSA. Each reconstructed record corresponds to a distinct oscillation with limited harmonic content.

MEM Spectra: 2.5 yr: QBO; 4-6 yr: ENSO

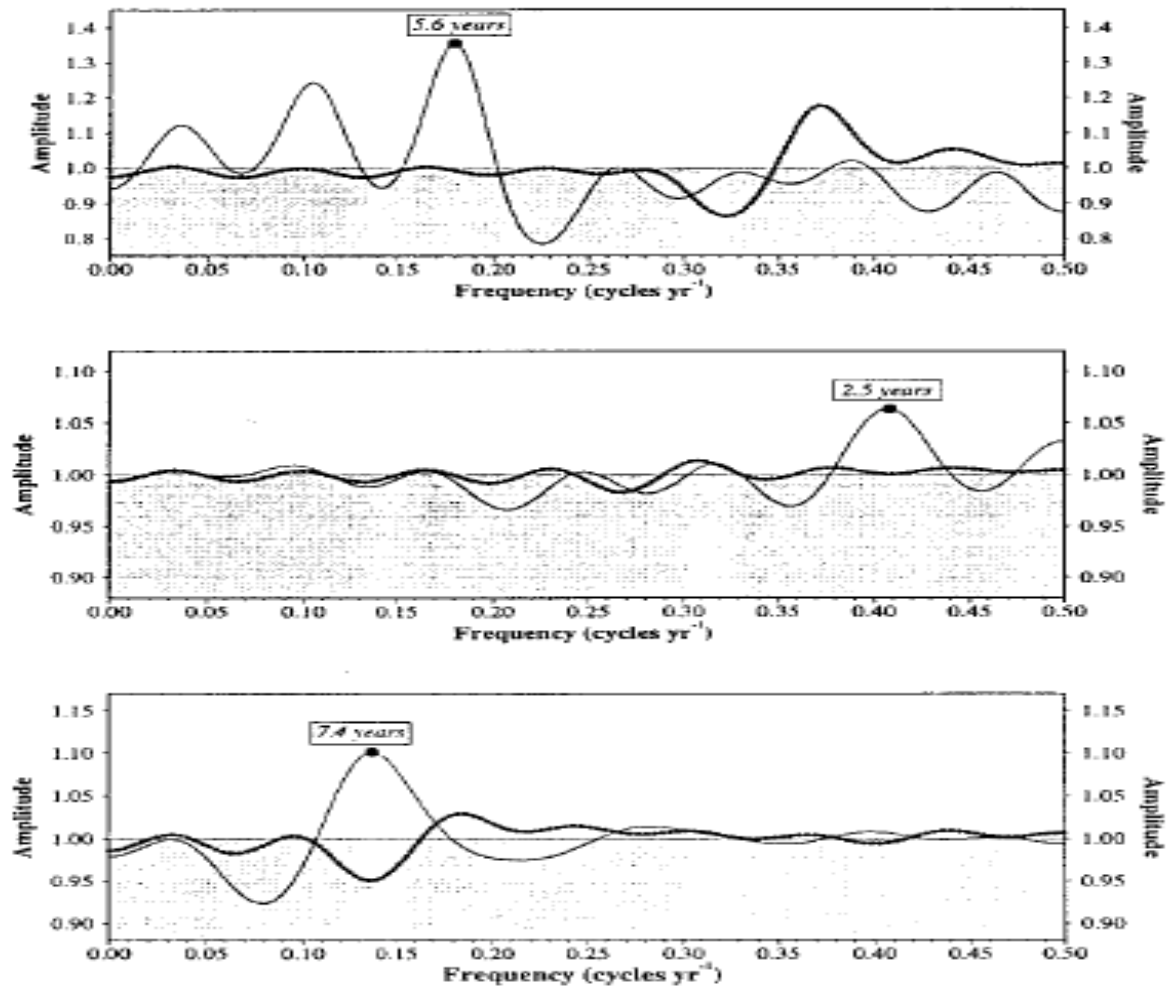


FIG. 6. MEM spectra of the three dominant reconstructed components of the detrended North Atlantic hurricane record using a maximum order of 15. The solid circle indicates the dominant frequency in the record. The thick lines correspond to the MEM of the three dominant reconstructed components of a permuted hurricane record. The ordinate scales are not identical across the graphs.

Composite Analysis of QBO and NA Hurricane Frequency

TABLE 1. Years of extreme QBO east and west phases over the period 1950–96 as determined by the upper-level (50 mb) zonal winds averaged from stations over the Caribbean from August through October, along with the corresponding components of North Atlantic hurricane activity. Q50 refers to the 50-mb zonal wind anomaly in m s^{-1} .

QBO east phase					QBO west phase				
Year	Q50	All	TO	BE	Year	Q50	All	TO	BE
1952	-11.2	6	6	0	1955	7.5	9	9	0
1954	-13.2	8	5	3	1957	8.5	3	2	1
1956	-7.8	4	3	1	1959	8.5	7	1	6
1968	-9.2	5	1	4	1961	7.5	8	7	1
1970	-10.2	5	1	4	1964	10.5	6	5	1
1972	-9.2	3	0	3	1975	7.5	6	4	2
1977	-12.5	5	1	4	1978	8.8	5	2	3
1984	-13.8	5	0	5	1980	8.2	9	4	5
1992	-9.8	4	0	4	1985	9.8	7	4	3
1994	-13.8	3	1	2	1995	10.8	11	9	2
Avg	-11.1	4.8	1.8	3.0	Avg	8.8	7.1	4.7	2.4

Composite analysis of ENSO and US Hurricane

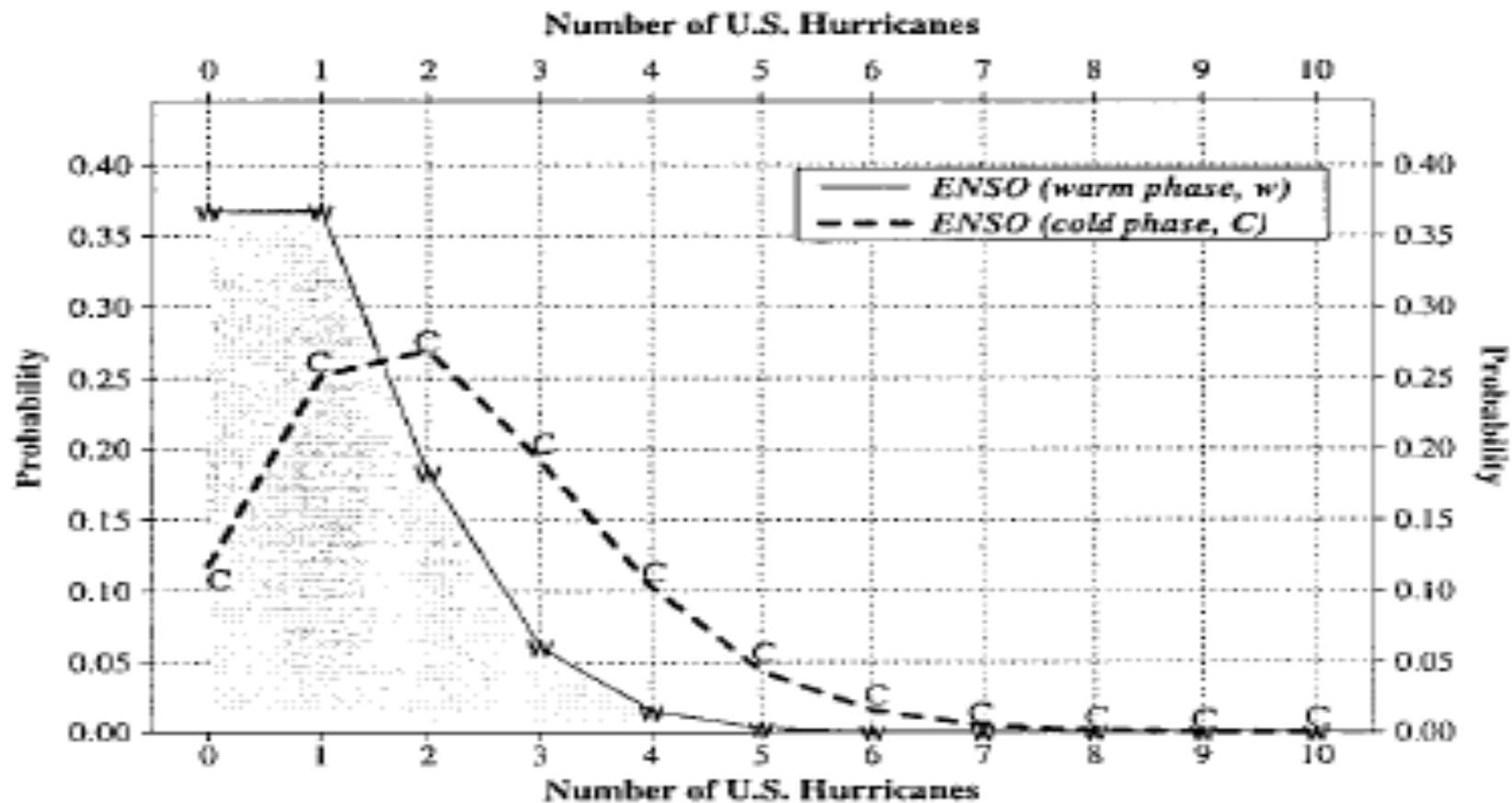


FIG. 10. Probability distributions of U.S. hurricanes with respect to the two phases of ENSO based on the assumption of the occurrence of U.S. hurricanes as a Poisson process. The Poisson parameter is estimated from data over the period 1869–1996. Note that, although overall U.S. hurricanes are more likely during a cold phase, the probability of exactly one U.S. hurricane is higher during a warm phase.

Solar Activity and Hurricane Frequency

TABLE 3. Years of extremes in the solar cycle over the period 1886–1996 as measured by the annual-averaged Wolf Sunspot Numbers (R_z) and the corresponding number of North Atlantic hurricanes by type.

10 maximum years					10 minimum years				
Year	R_z	All	TO	BE	Year	R_z	All	TO	BE
1947	151.6	5	5	0	1888	6.8	5	3	2
1956	141.7	4	3	1	1889	6.3	5	4	1
1957	190.2	3	2	1	1901	2.7	3	2	1
1958	184.8	7	7	0	1902	5.0	3	3	0
1959	159.0	7	1	6	1911	5.7	3	3	0
1979	155.4	5	2	3	1912	3.6	4	1	3
1980	154.6	9	4	5	1913	1.4	3	1	2
1989	157.7	7	5	2	1923	5.8	3	2	1
1990	141.8	8	3	5	1933	5.7	10	10	0
1991	145.2	4	0	4	1954	4.4	8	5	3
Avg.	158.2	5.9	3.2	2.7	Avg.	4.7	4.7	3.4	1.3

probably safe to conclude that if there is any relationship between solar output and North Atlantic hurricane climate, as this and other analyses hint at, it is likely through BE hurricane activity.

CISK (Conditional Instability of the Second Kind) Theory (1960's – 1970's)

Represents a cooperation between convection and large-scale convergence:

- Weak disturbances containing vorticity
- Ekman layer (BL) convergence through Ekman pumping
- Increased convection
- Latent heat release
- Temperature increase
- Sfc pressure falls
- Increased vorticity
- Increased convergence
- A feedback loop - instability

Linear analysis to capture the above instability process has not been very successful, however, since there is little evidence that such interaction leads to a growth rate maximum on the observed scale of hurricanes.

Hurricane as a Carnot Engine (Emanuel, 1987)

Air-Sea Interaction Theory

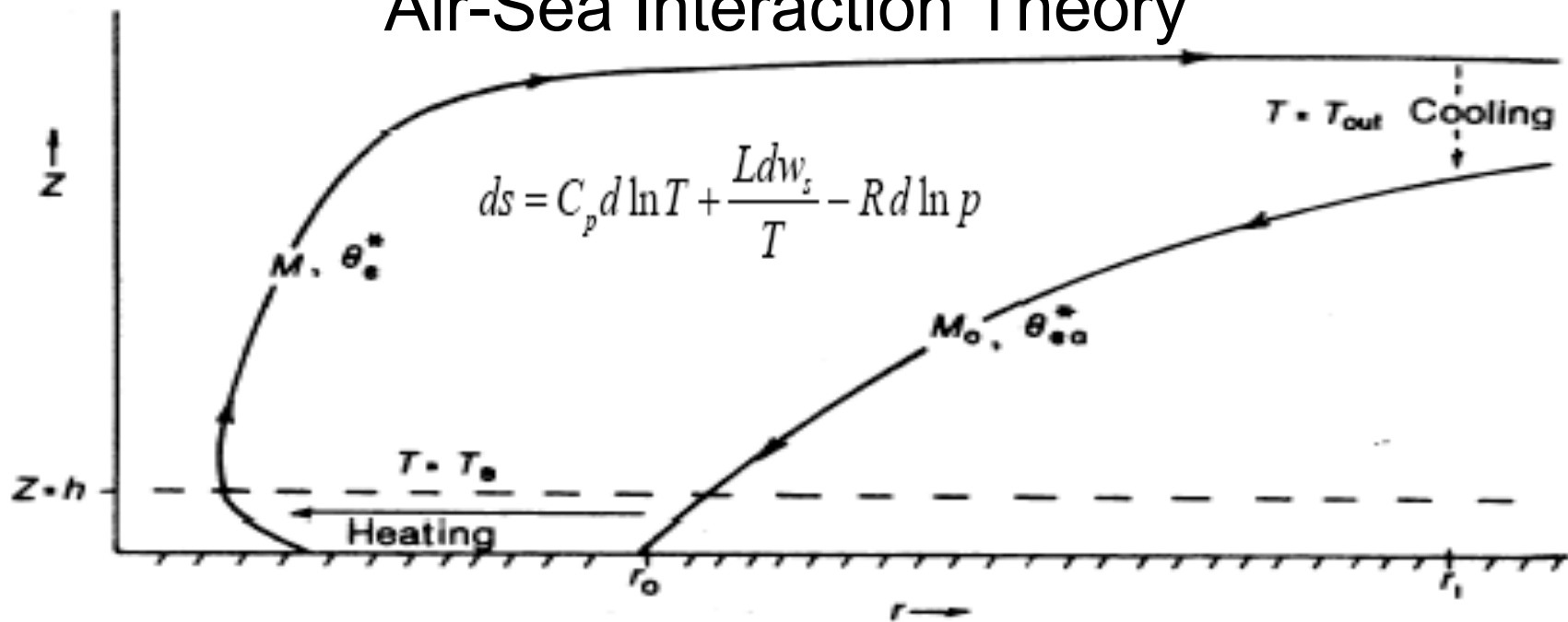


Fig. 1 Carnot cycle of the mature tropical cyclone³. Air begins with absolute angular momentum per unit mass M_0 and moist entropy θ_{ea}^* at a radius r_0 , and flows inward at constant temperature T_B within a thin boundary layer, where it loses angular momentum and gains moist entropy from the sea surface. It then ascends and flows outward to large radii, preserving its angular momentum (M) and moist entropy (θ_e^*). Eventually, at large radii, the air loses moist entropy by radiative cooling to space at a mean temperature T_{out} and acquires angular momentum by interaction with the environment.

Knowledge of the frictional loss in the boundary layer can be used to calculate the total drop in pressure in towards the eye of the storm through the use of Bernoulli's energy equation, which may be written

$$\frac{1}{2}\Delta v^2 + \int \alpha dp + W_{BL} = 0 \quad (2)$$

where $\frac{1}{2}\Delta v^2$ is the total change in kinetic energy per unit mass following the air flowing inward in the boundary layer, α is the volume per unit mass and p is the pressure. Since v is approximately zero at the beginning of the inflow (at r_0) and is exactly zero at $r = 0$, Bernoulli's equation integrated all the way into the centre of the storm may be expressed

$$\int_{r_0}^0 \alpha dp = -\epsilon \Delta Q, \quad (3)$$

where we have used equation (1) for W_{BL} . Using the ideal gas law to express α as a function of p and T (and water vapour content, which is variable), the author³ showed that the integral in equation (3) can be evaluated exactly. Specifically, both α and ΔQ can be regarded as functions of temperature, pressure and relative humidity (RH), so that equation (3) has the functional form

$$\Delta G(p, T, RH) = \epsilon \Delta F(p, T, RH) \quad (4)$$

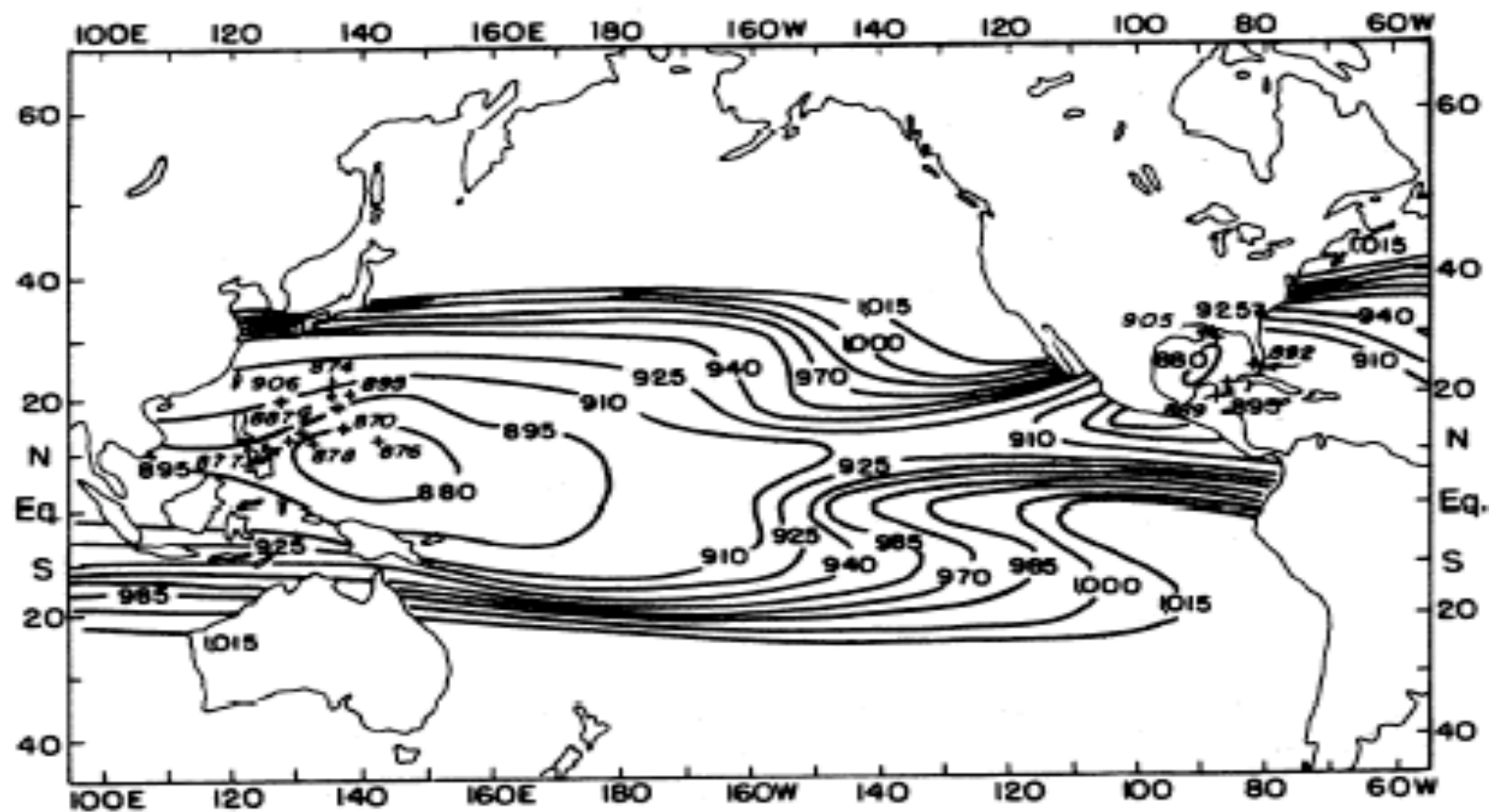
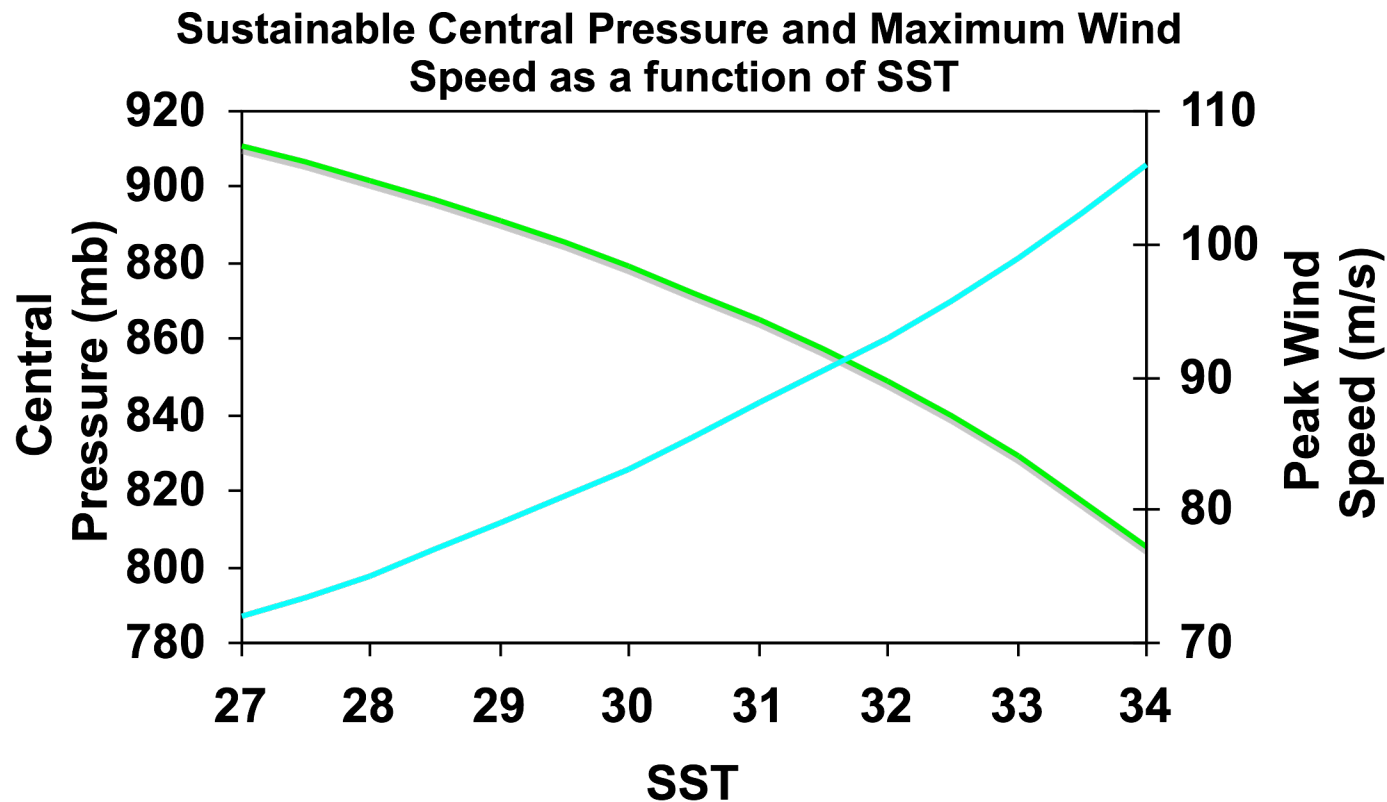


Fig. 2 Minimum sustainable central pressures (mb) under September mean climatological conditions, assuming an ambient pressure of 1,015 mb (ref. 3). Crosses mark the positions and central pressures of some of the most intense tropical cyclones on record¹.

- Assume Carnot efficiency, calc. using tropospheric temperature structure
- Assume fixed relative humidity
- Sensitive to SST since latent heat at fixed RH is an exponential fn of SST—doubling for every 10 C rise. About 5% increase in wind speed per deg C

Table 1 Minimum sustainable central pressure and maximum wind speed as a function of sea surface temperature with $\varepsilon = 0.33$ and an ambient relative humidity of 78%. (Ambient pressure = 1,015 mbar)

T (°C)	P_c (mbar)	V_{\max} (m s ⁻¹)
27	911	72
28	902	75
29	891	79
30	879	83
31	865	88
32	849	93
33	829	99
34	805	106



- Wind increases as square root of pressure drop
- Peak wind increases by about 5% per °C
- Observed increase in SST of 0.5° C implies about 2.5% increase in peak wind
- Destructive potential varies as sq. of wind speed or as pressure drop

Synopsis of Emanuel 1986-88

- Potential intensity (max wind speed) depends on SST
- Destructive potential proportional to sq of wind speed
- Used 2.8—4.3 C increase in tropical SST from GSFC 2xCO₂ simulations
- Concluded that hurricane intensities are likely to increase due to global warming
- Caveats
 1. Only a small fraction of cyclones reach the maximum intensity: Latent heat flux depends strongly on wind speed and that needs to be rather high—well developed vortex—for hurricane to form
 2. Climate change simulations were rather crude

Considerations in Emanuel 2005

- With observed warming of the tropics of around 0.5° C, predicted changes in intensity (~2.5%) are too small to have been observed.
- Since potential intensity is sensitive to the difference between SST and average tropospheric temperature, regional fluctuations in SST more important than global trends
- Considers power dissipation in individual basins

$$PD = 2\pi \int_0^{\tau} \int_0^{r_0} C_D \rho |V|^3 r dr dt$$

$$PDI \equiv \int_0^{\tau} V_{\max}^3 dt$$

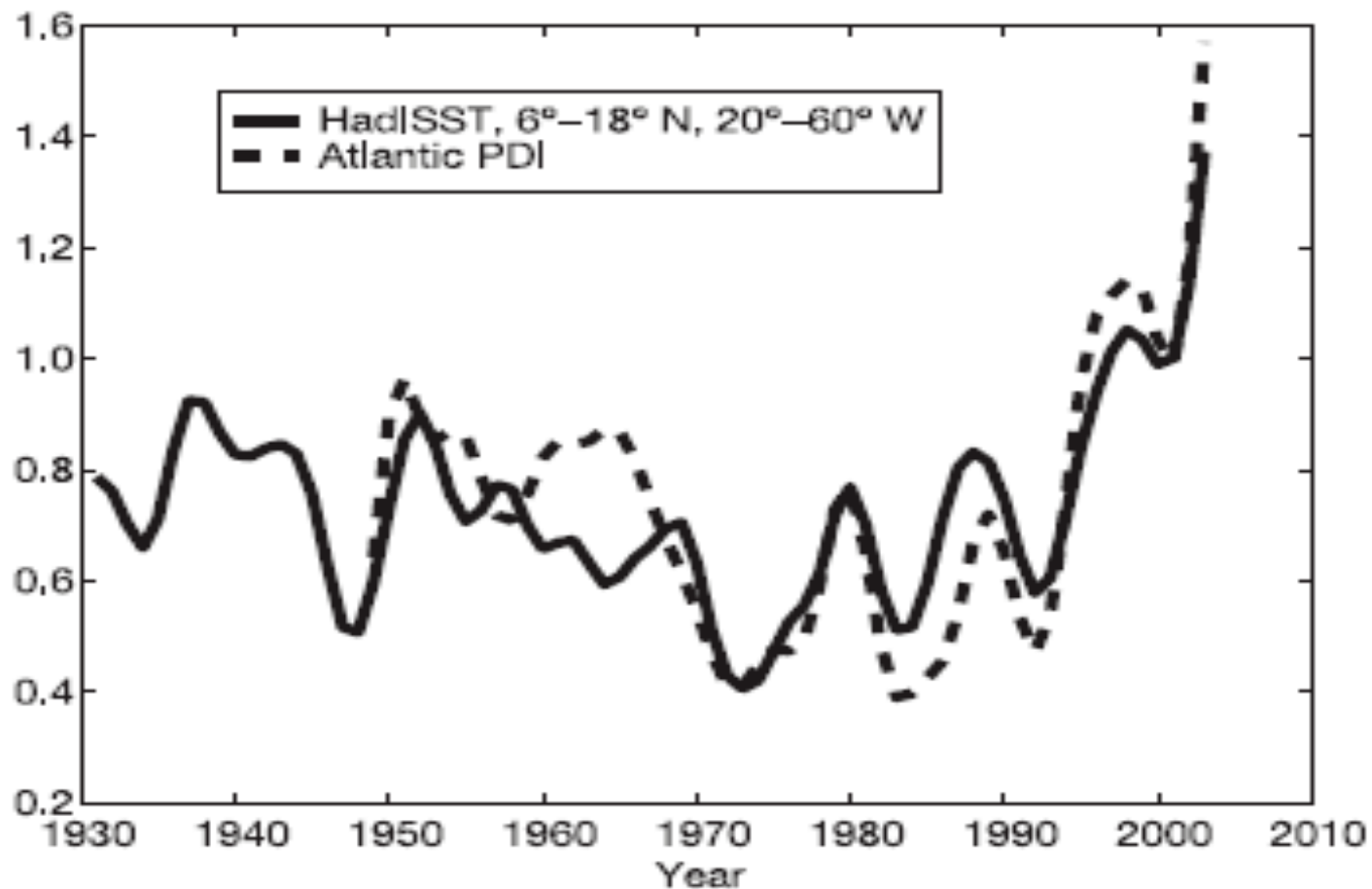


Figure 1 | A measure of the total power dissipated annually by tropical cyclones in the North Atlantic (the power dissipation index, PDI) compared to September sea surface temperature (SST). The PDI has been multiplied by 2.1×10^{-12} and the SST, obtained from the Hadley Centre Sea Ice and SST data set (HadISST)²², is averaged over a box bounded in latitude by 6° N and 18° N, and in longitude by 20° W and 60° W. Both quantities have been smoothed twice using equation (3), and a constant offset has been added to the temperature data for ease of comparison. Note that total Atlantic hurricane power dissipation has more than doubled in the past 30 yr.

NA Hurricane PDI vs. Sep SST

- Correlation of 0.65 suggests SST control of PDI in North Atlantic
- Influence of ENSO, NAO, Atlantic multi-decadal mode may be seen
- No QBO signal because of averaging
- Unprecedented large upswing in last decade probably related to global warming
- PDI more than doubled over past 30 yrs
- Note 3rd power of V in PDI (essentially 4th)

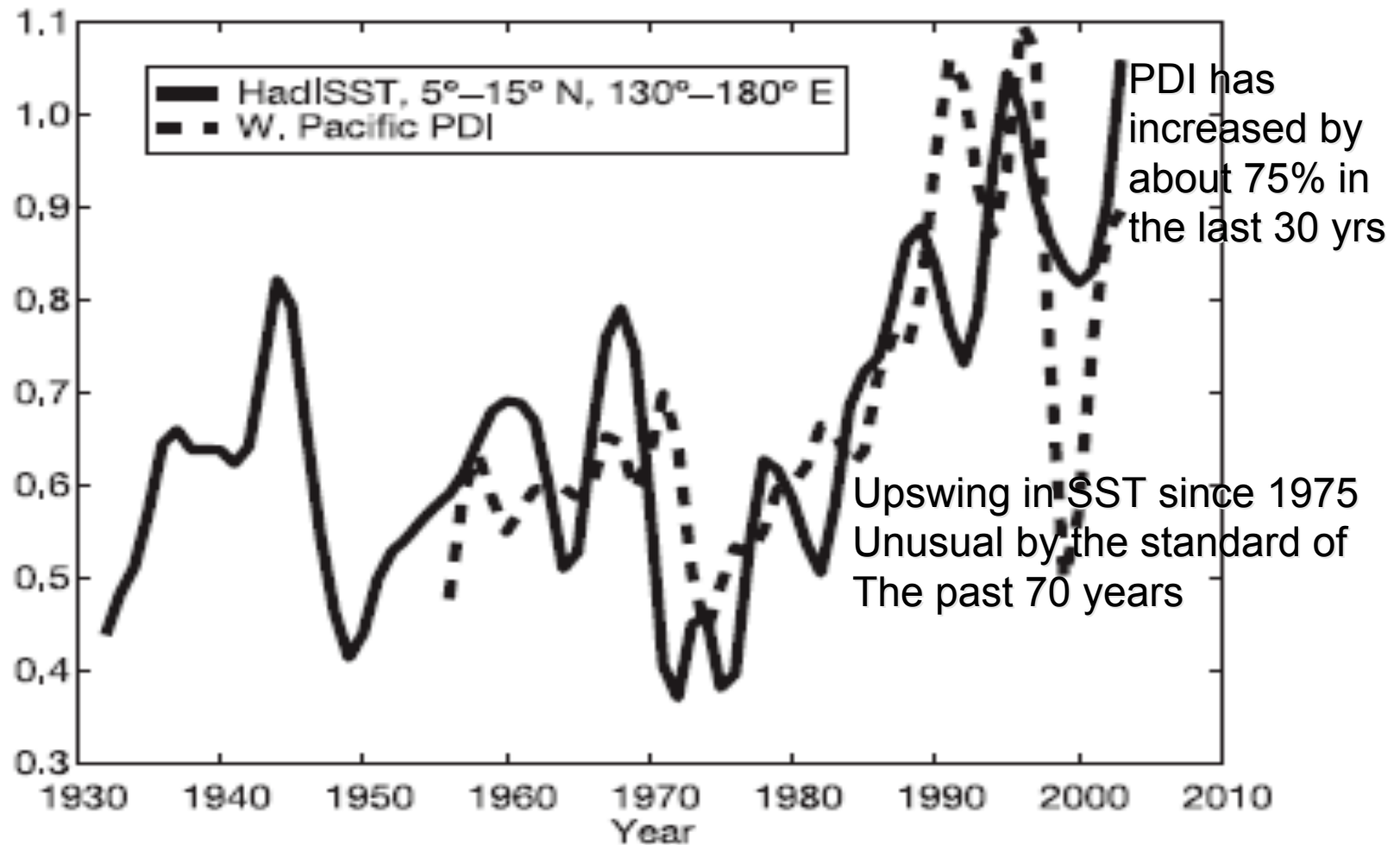


Figure 2 | Annually accumulated PDI for the western North Pacific, compared to July–November average SST. The PDI has been multiplied by a factor of 8.3×10^{-13} and the HadISST (with a constant offset) is averaged over a box bounded in latitude by 5° N and 15° N, and in longitude by 130° E and 180° E. Both quantities have been smoothed twice using equation (3). Power dissipation by western North Pacific tropical cyclones has increased by about 75% in the past 30 yr.

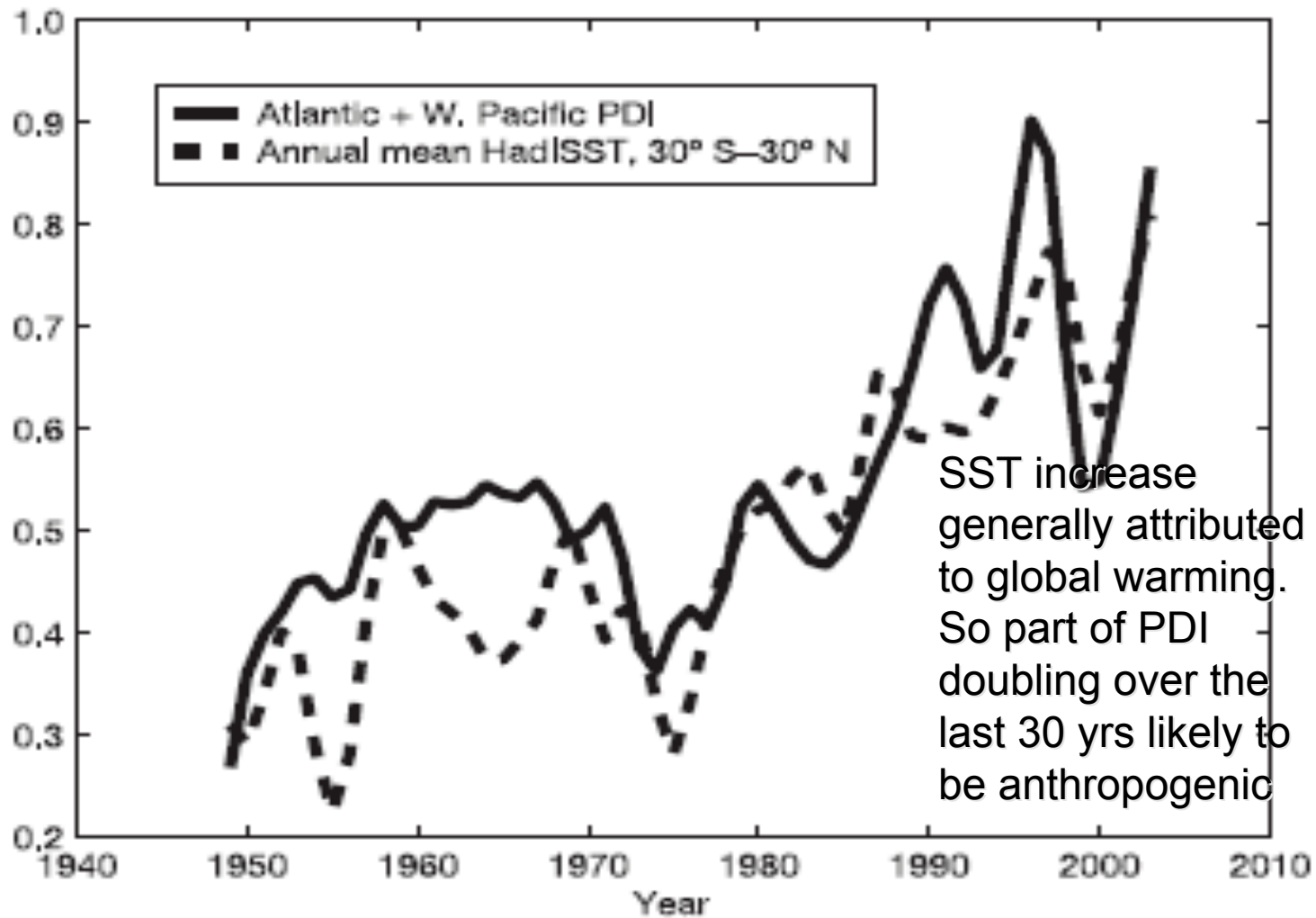


Figure 3 | Annually accumulated PDI for the western North Pacific and North Atlantic, compared to annually averaged SST. The PDI has been multiplied by a factor of 5.8×10^{-13} and the HadISST (with a constant offset) is averaged between 30° S and 30° N. Both quantities have been smoothed twice using equation (3). This combined PDI has nearly doubled over the past 30 yr.

Synopsis of Emanuel 2005

- Total power dissipated over lifetime has increased by >50% since 1970s
- Greater storm intensities—annual average storm peak wind speeds have doubled (c.f. Webster 2005)
- Longer lifetime assuming fixed growth rate—accumulated annual duration in NA and WP has increased about 60%
- Correlated to tropical SST
- SST increase in the last 30 years generally attributed to global warming and so at least part of the PDI increase is likely anthropogenic

Synopsis of Emanuel 2005

- Theory—5% increase of wind per deg C rise of SST—so wind should have increased by 2-3% and PD by 6-9%. With longer storms 8-12%
- However, reanalysed data indicates that the potential maximum wind speed (intensity) has gone up by 10% and so PD by about 40%.
- Potential intensity is sensitive to the difference between SST and average tropospheric temperature, and the observed atmospheric temperature does not keep pace with SST.
- Increased subsurface T in ocean leading to reduced feedback; decrease in wind shear (small)
- Increased power dissipation—increased vertical diffusivity—increased THC?

Analysis of Webster 2005

- Satellite era 1970-2004
- Frequency, Intensity, Duration
 - Storm days
 - Hurricane days
 - Cyclone days

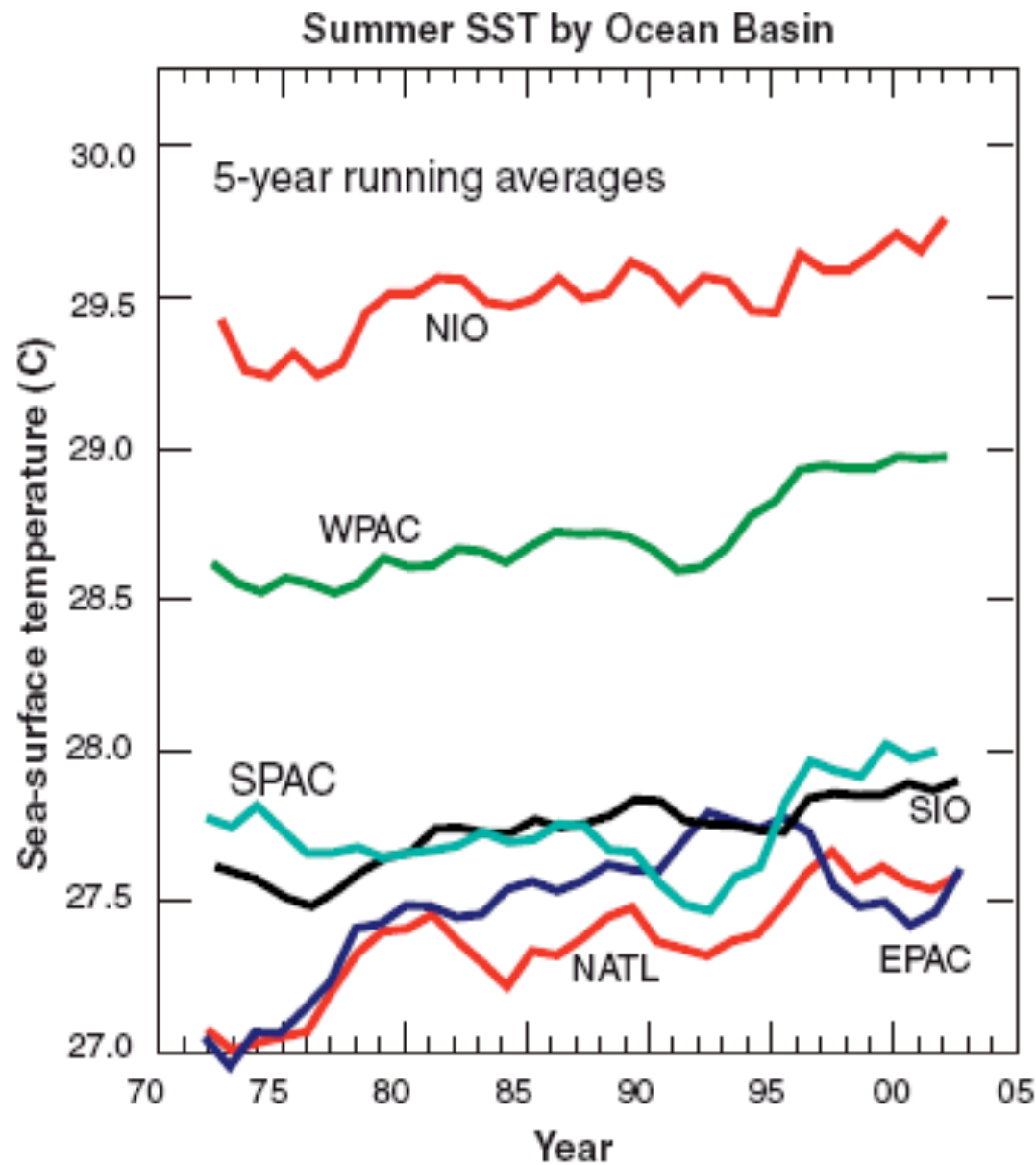


Fig. 1. Running 5-year mean of SST during the respective hurricane seasons for the principal ocean basins in which hurricanes occur: the North Atlantic Ocean (NATL: 90° to 20°E, 5° to 25°N, June-October), the Western Pacific Ocean (WPAC: 120° to 180°E, 5° to 20°N, May-December), the East Pacific Ocean (EPAC: 90° to 120°W, 5° to 20°N, June-October), the Southwest Pacific Ocean (SPAC: 155° to 180°E, 5° to 20°S, December-April), the North Indian Ocean (NIO: 55° to 90°E, 5° to 20°N, April-May and September-November), and the South Indian Ocean (SIO: 50° to 115°E, 5° to 20°S, November-April).

Webster 2005

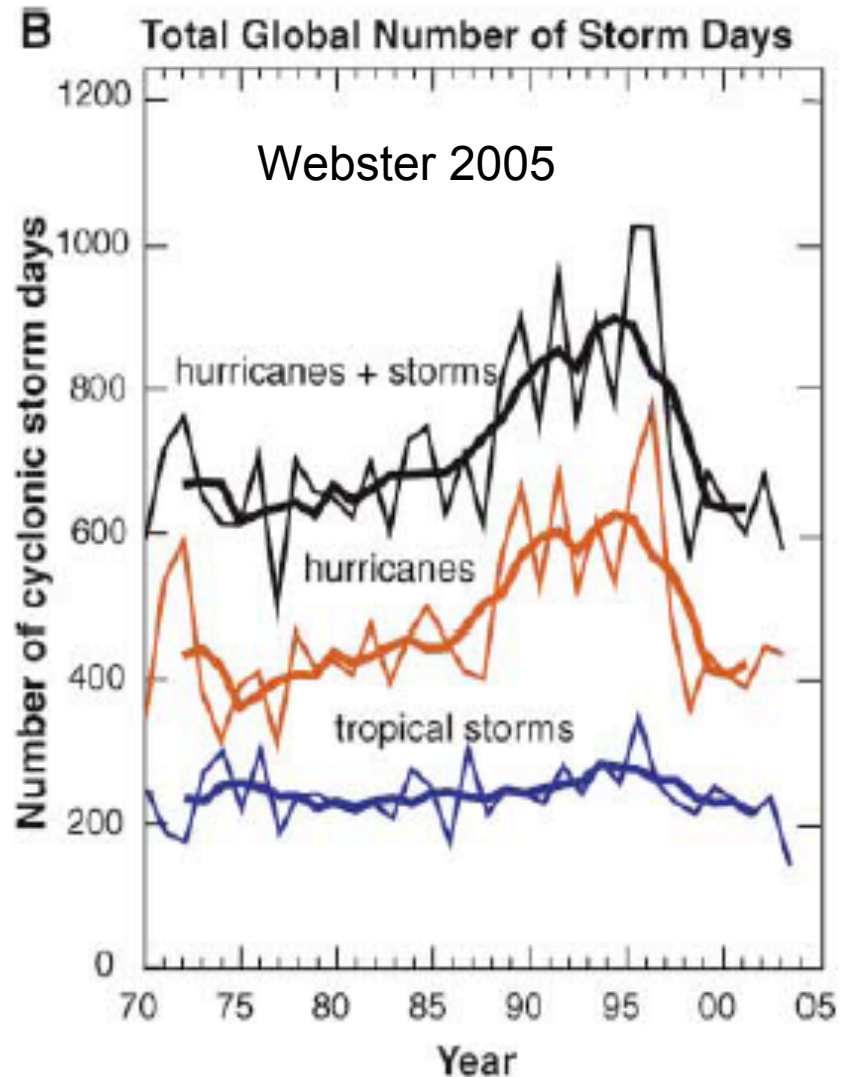
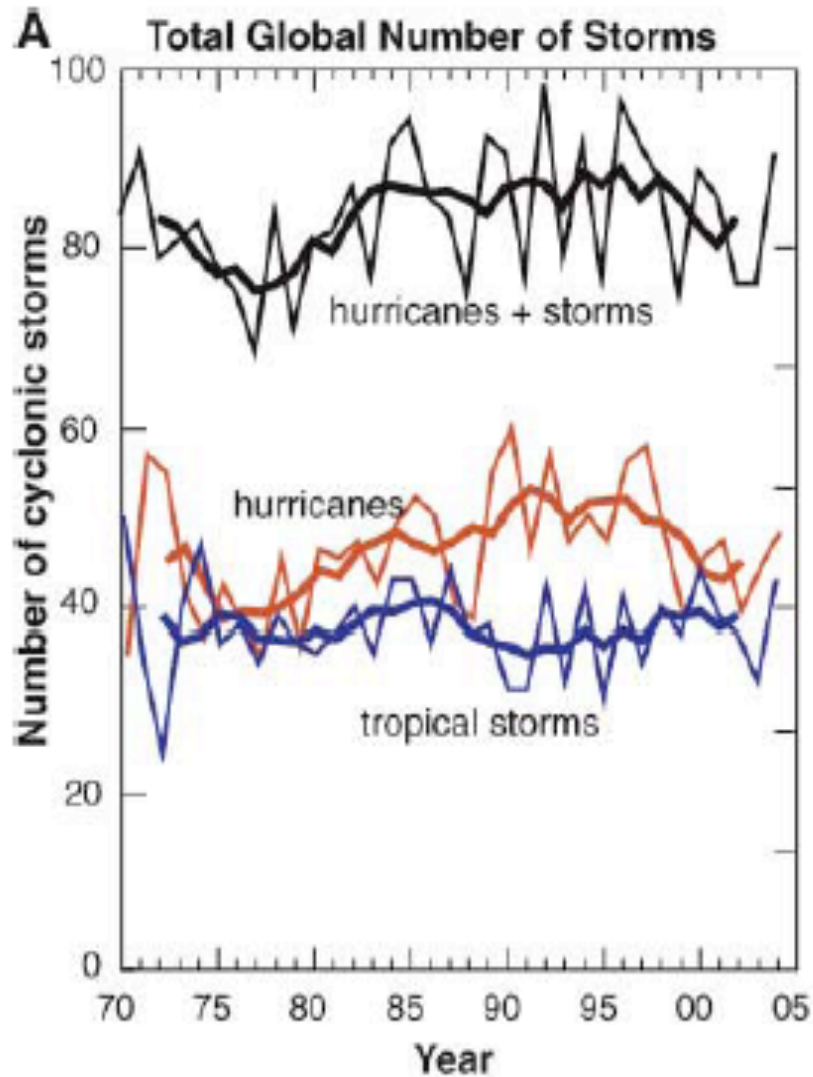


Fig. 2. Global time series for 1970–2004 of (A) number of storms and (B) number of storm days for tropical cyclones (hurricanes plus tropical storms; black curves), hurricanes (red curves), and tropical storms (blue curves). Contours indicate the year-by-year variability, and the bold curves show the 5-year running average.

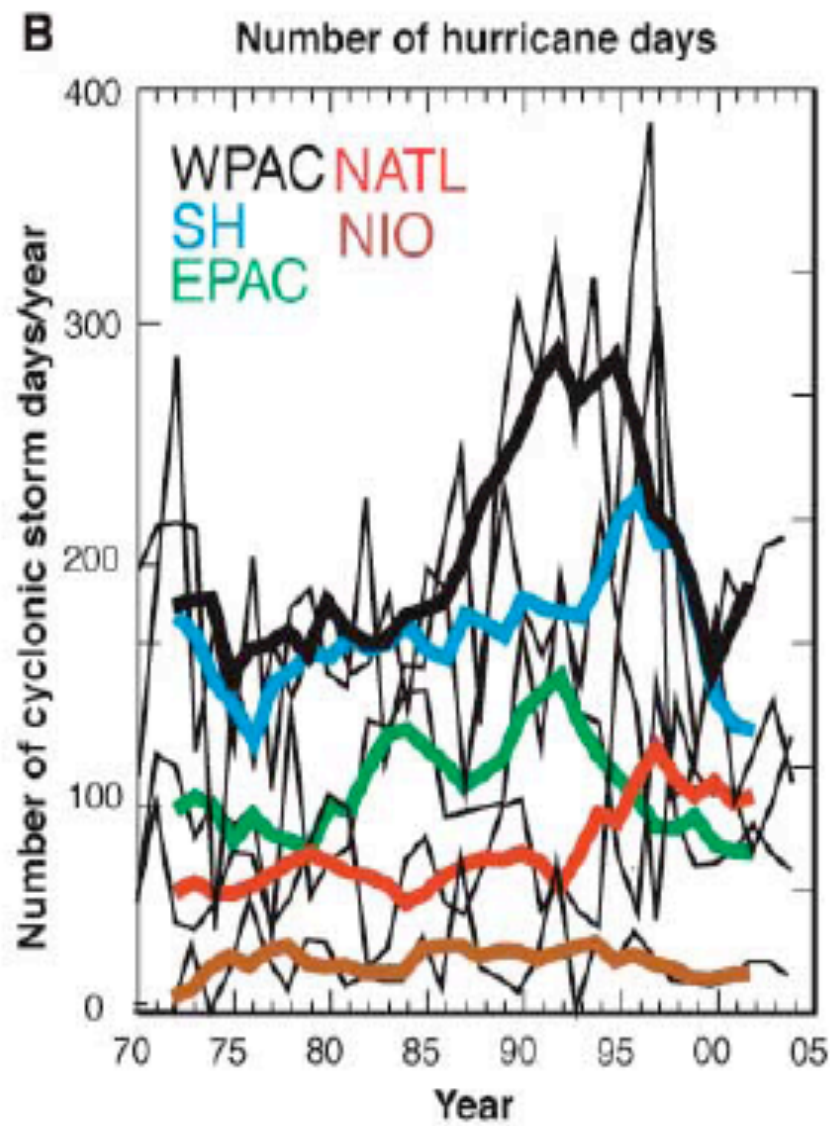
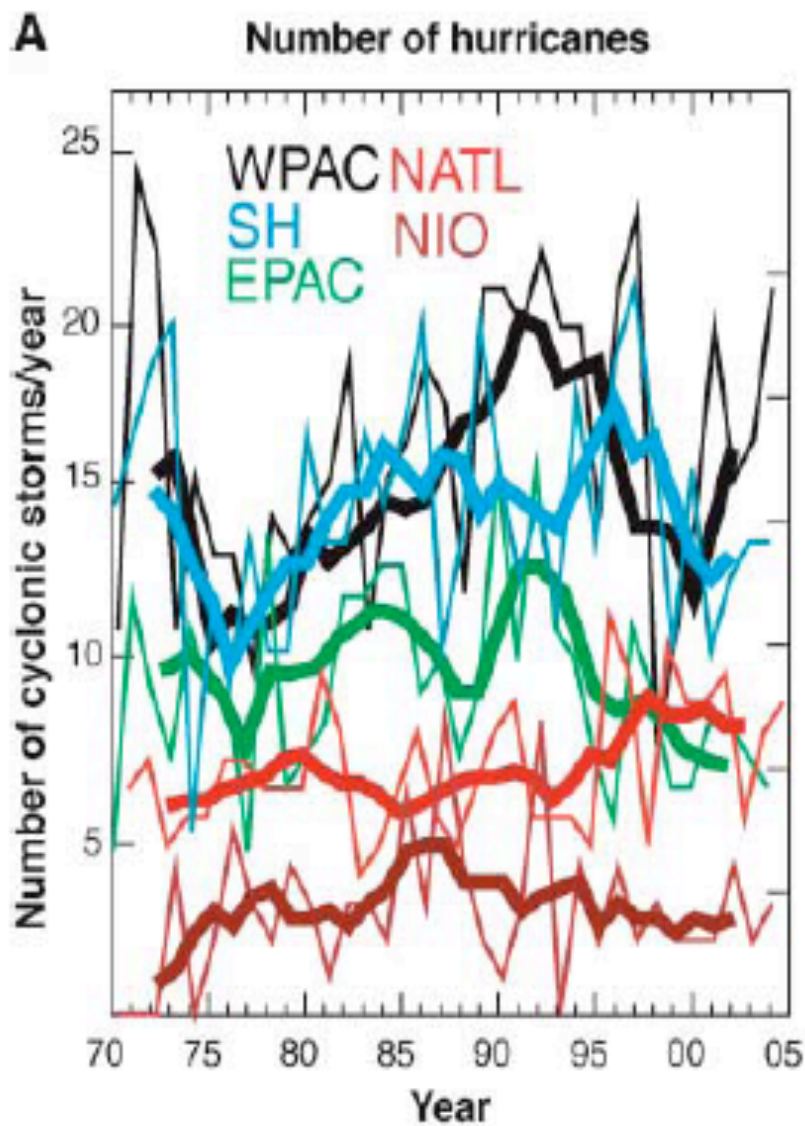


Fig. 3. Regional time series for 1970–2004 for the NATL, WPAC, EPAC, NIO, and Southern Hemisphere (SIO plus SPAC) for (A) total number of hurricanes and (B) total number of hurricane days. Thin lines indicate the year-by-year statistics. Heavy lines show the 5-year running averages.

Frequency and Duration vs. SST (Webster 2005)

- No discernable trend in either frequency or duration either globally or regionally
- Exception to above is North Atlantic, where both duration and frequency positively correlated to SST
- However, in Pacific (both eastern and western), duration and frequency of typhoons not well correlated to SST

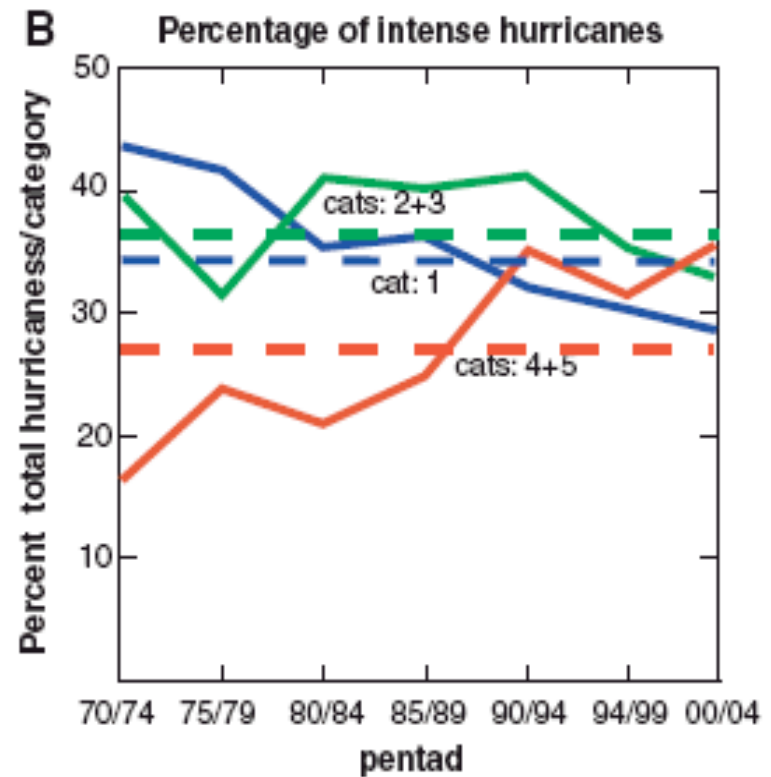
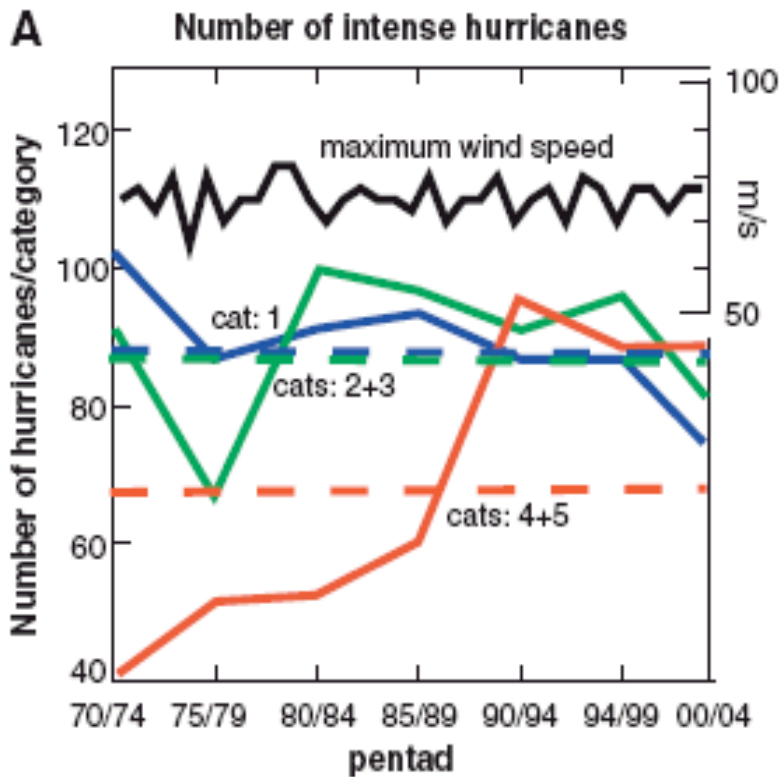


Fig. 4. Intensity of hurricanes according to the Saffir-Simpson scale (categories 1 to 5). (A) The total number of category 1 storms (blue curve), the sum of categories 2 and 3 (green), and the sum of categories 4 and 5 (red) in 5-year periods. The bold curve is the maximum hurricane wind speed observed globally (measured in meters per second). The horizontal dashed lines show the 1970–2004 average numbers in each category. (B) Same as (A), except for the percent of the total number of hurricanes in each category class. Dashed lines show average percentages in each category over the 1970–2004 period.

Table 1. Change in the number and percentage of hurricanes in categories 4 and 5 for the 15-year periods 1975–1989 and 1990–2004 for the different ocean basins.

Basin	Period			
	1975–1989		1990–2004	
	Number	Percentage	Number	Percentage
East Pacific Ocean	36	25	49	35
West Pacific Ocean	85	25	116	41
North Atlantic	16	20	25	25
Southwestern Pacific	10	12	22	28
North Indian	1	8	7	25
South Indian	23	18	50	34

Intensity and Distribution vs. SST (Webster 2005)

- Cat 4/5 hurricanes have increased both in number and proportion
- Maximum wind speeds have stayed put
- Consistent with Emanuel 2005—annual average storm peak wind speeds has increased by about 50%
- Cat 1 hurricanes have remained the same in number, but decreased in proportion (wrong?)

- In summary, careful analysis of global hurricane data shows that, against a background of increasing SST, **no global trend has yet emerged in the number of tropical storms and hurricanes.**
- We conclude that global data indicate a 30-year trend toward **more frequent** and intense hurricanes (should be 'more frequent intense hurricanes'?)

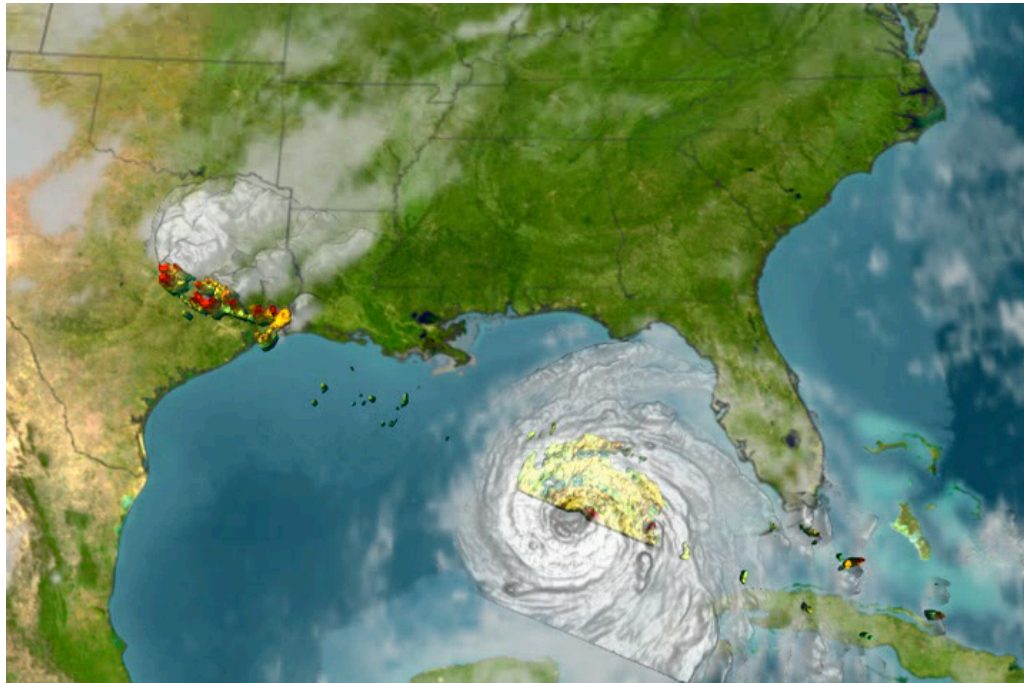
Is global warming causing a change in hurricane variability?

- No discernable trend in frequency
- Suggestions that more intense storms are getting more frequent

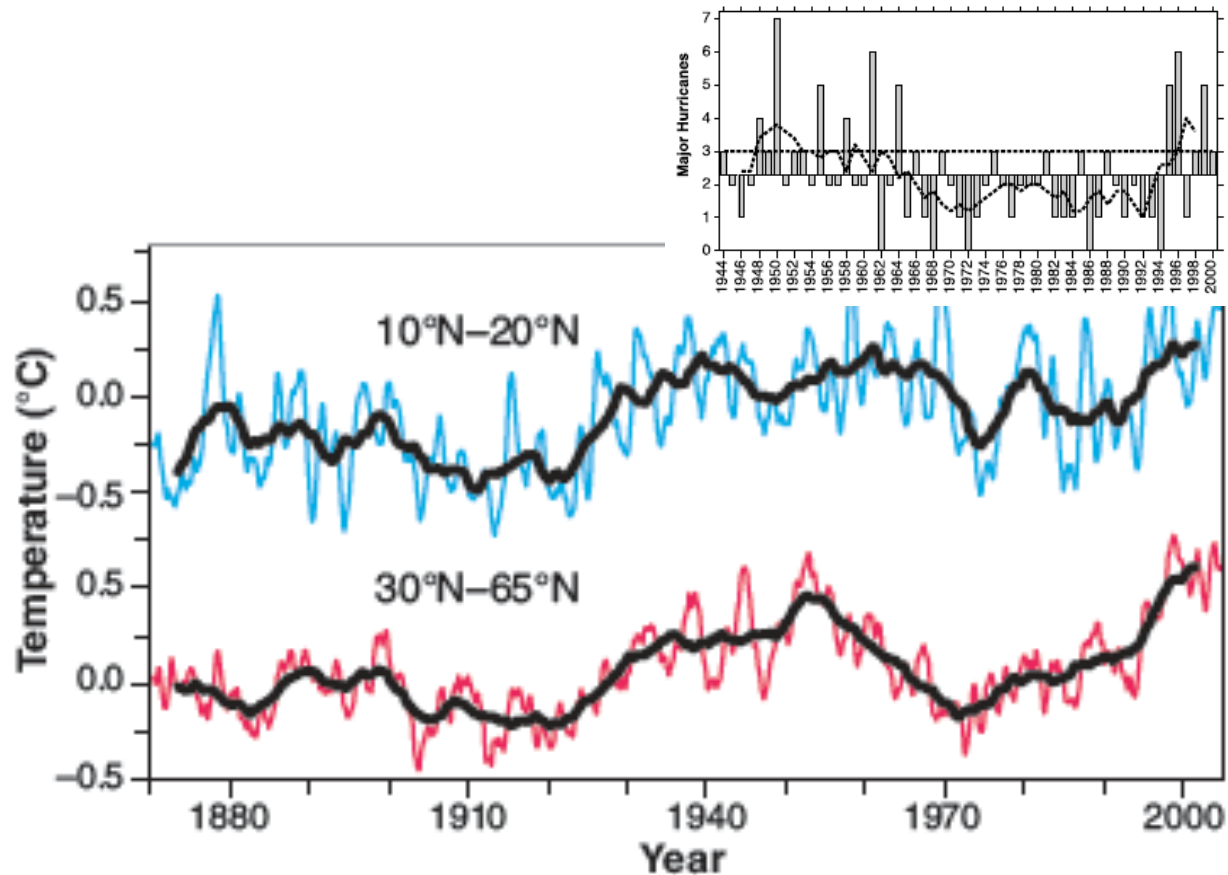
The Price of Policy

- A sobering fact is that Population and Societal Trends have overwhelming influence
- Pielke 2004 suggest that for every \$ in coastal damage produced by climate change societal trends are going to produce \$22--\$60 in additional damage

Katrina Aug 28; TRMM Precip Radar (NASA)

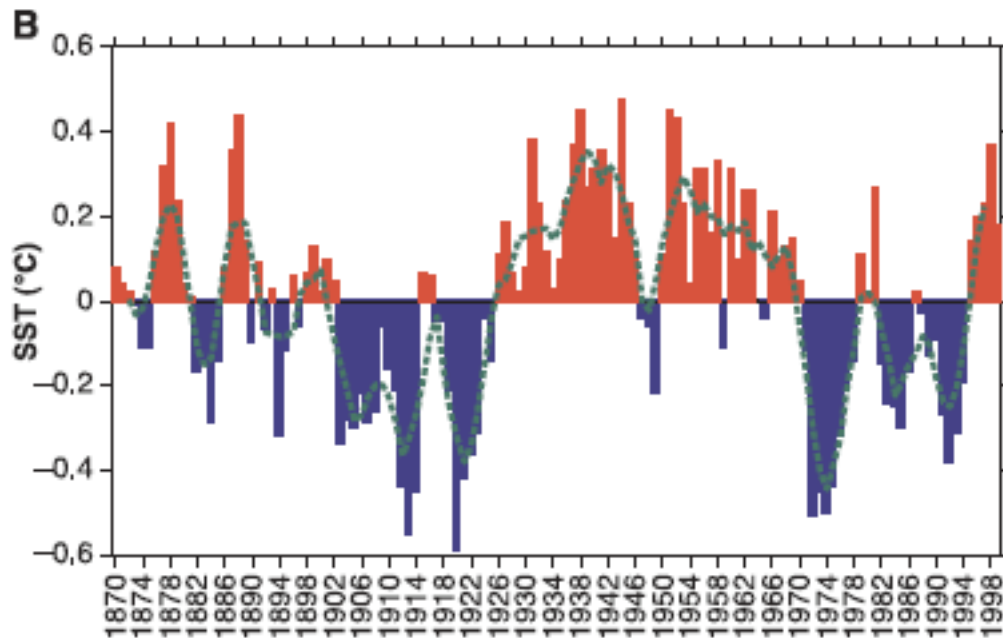
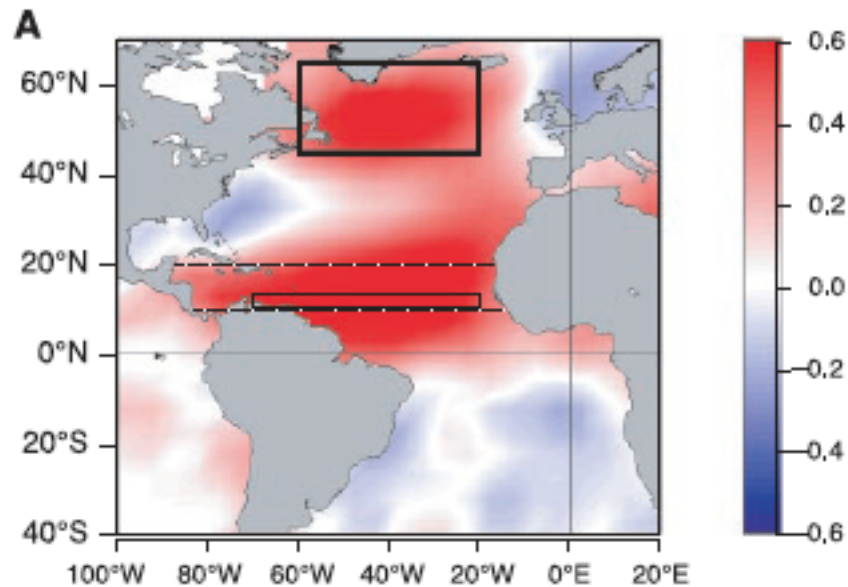


AMO: Interdecadal Variability in SST (Goldenberg 01, Trenberth 05)



Getting warmer. Annual mean SST anomalies relative to 1961 to 1990 (23) for 1870 to 2004, averaged over the tropical Atlantic (10°N to 20°N, excluding the Caribbean west of 80°W) (**top**) and the extratropical North Atlantic (30°N to 65°N) (**bottom**). Heavy lines are 10-year running means.

The Atlantic Multidecadal Oscillation (Goldenberg et al., 2001)



Atlantic sector of the first rotated EOF of non-ENSO global SST variability for 1870-2000 referred to as the atlantic multi-decadal mode (38, 39). (A) Spatial distribution of correlations between local monthly SST anomalies and the modal reconstruction over the indexed region (northern rectangle), the general area where the mode amplitude is the strongest. This distribution has a similar spatial structure to the actual rotated EOF and gives a measure of the local fractional variance (squared temporal correlation) accounted for at each grid point. Dashed lines give north and south boundaries of main development region (MDR) and box (10 to 14N, 20 to 70W) is region used to calculate data for Fig. 3. (B) Temporal reconstruction (annual means) of the mode-related variability averaged over the rectangular area in (A). Dashed curved line is 5-year running mean. Although the signal is stronger in the North Atlantic, it is global in scope with positively correlated co-oscillations in parts of the North Pacific (55). For the multi-decadal variations shown here, the coherence between the MDR and far North Atlantic is a robust feature. The SST fluctuations in the far North Atlantic could be used as a proxy for changes in the MDR.

KNIGHT ET AL.: THC CYCLES IN OBSERVED CLIMATE

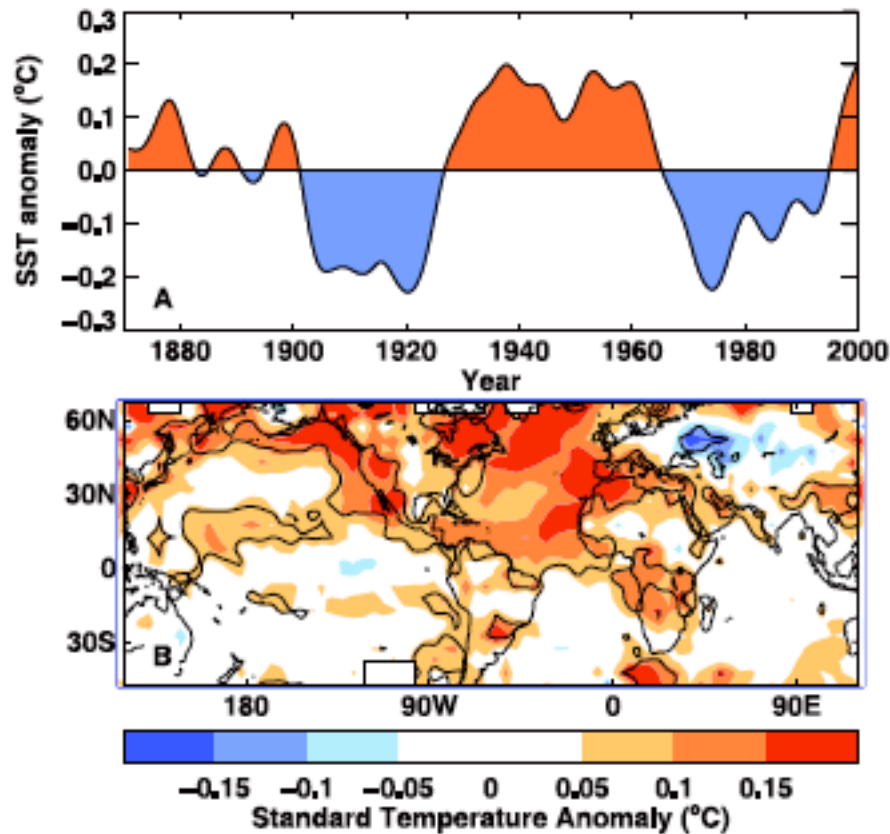


Figure 1. (a) AMO index derived from detrended area weighted mean North Atlantic SST anomalies by using a Chebyshev filter with a half-power period of 13.3 years. SST data are from the HadISST data set [Rayner et al., 2003]. (b) Surface temperature anomaly associated with one positive standard deviation of the AMO index, calculated by regression of surface temperatures with the index and scaled by its standard deviation. Combined land and sea-surface temperature data are from an optimally interpolated version of the HadCRUTv data set [Jones et al., 2001]. The solid contour bounds regions significant at the 90% limit of a two-sided t-test accounting for auto-correlation using the method of Folland et al. [1991].

KNIGHT ET AL., 2005

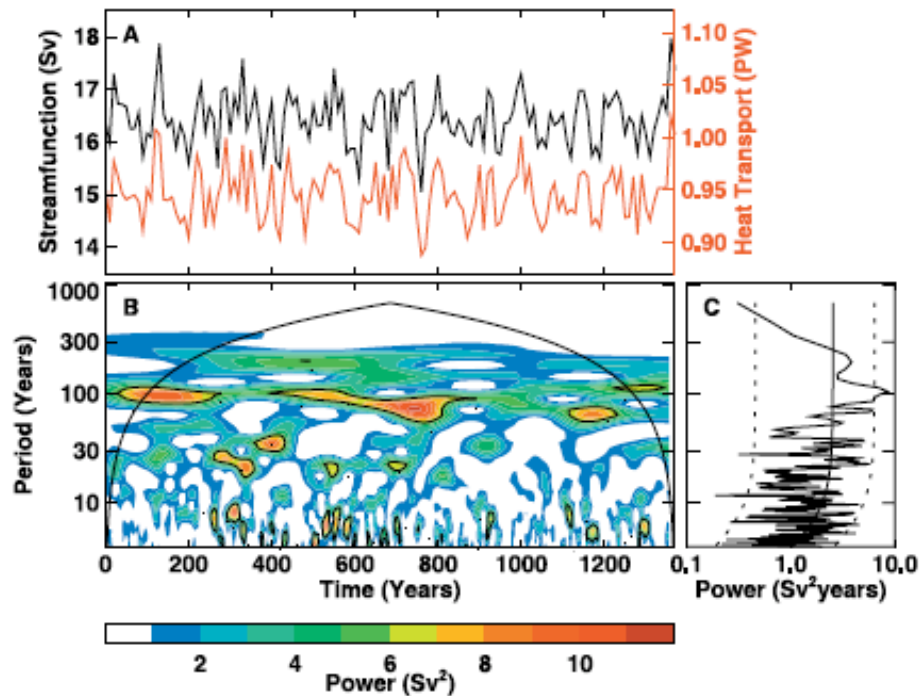


Figure 2. (a) Decadal mean THC index (black), and meridional heat transport at 30°N (red). (b) Wavelet analysis of the annual mean THC index using a continuous Morlet transform. Statistical significance at the 95% confidence interval is indicated by the contour. Curves bound the region where power is estimated from partial waves. (c) Power spectrum of the annual mean THC index. 95% confidence intervals are shown by the dashed curves.

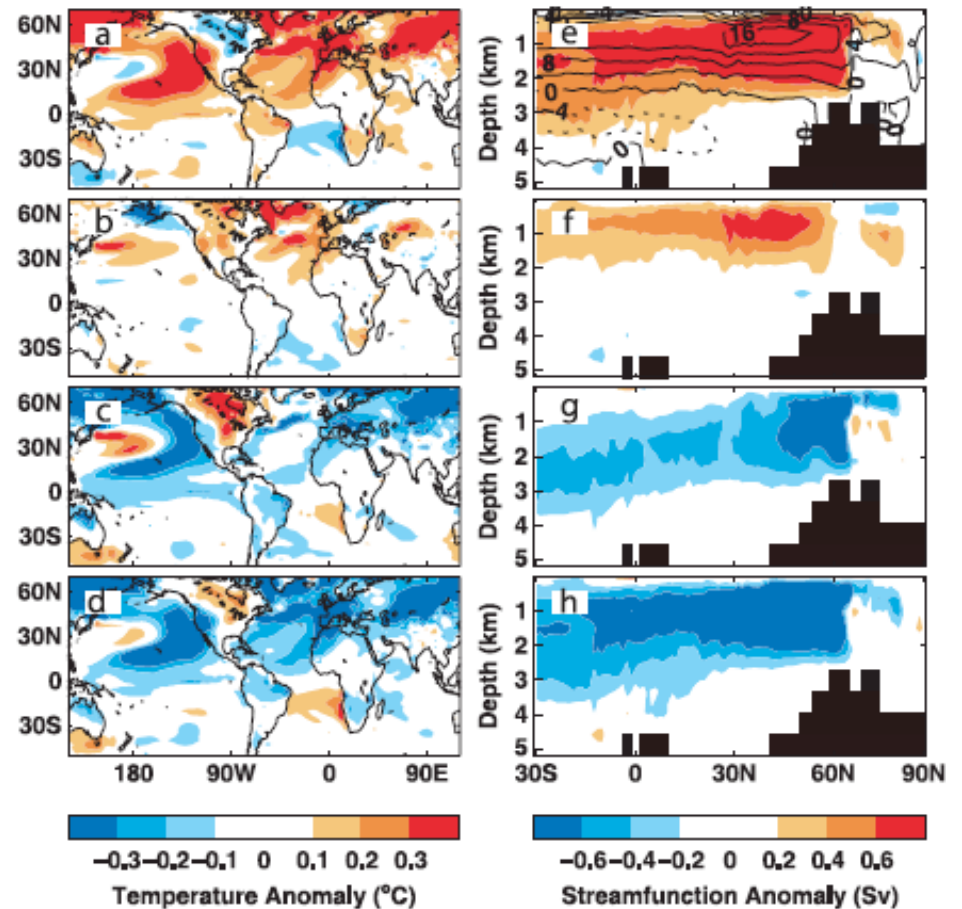


Figure 3. Joint MTM-SVD analysis of simulated decadal mean surface temperature and Atlantic overturning streamfunction for model years 400 to 900. Panels a–d show the signal in surface temperature anomaly in the frequency band from (70 years)¹ to (180 years)¹, at phases of 0, 60, 120, 180 respectively. Zero phase corresponds to maximum mean Northern Hemisphere temperature. Panels e–h show the corresponding phases of the covarying signal in streamfunction anomaly in the same band. In panel e, the climatological streamfunction is shown by contours, such that the mean THC and anomalous THC strength are positive (clockwise). Negative contours are dashed.

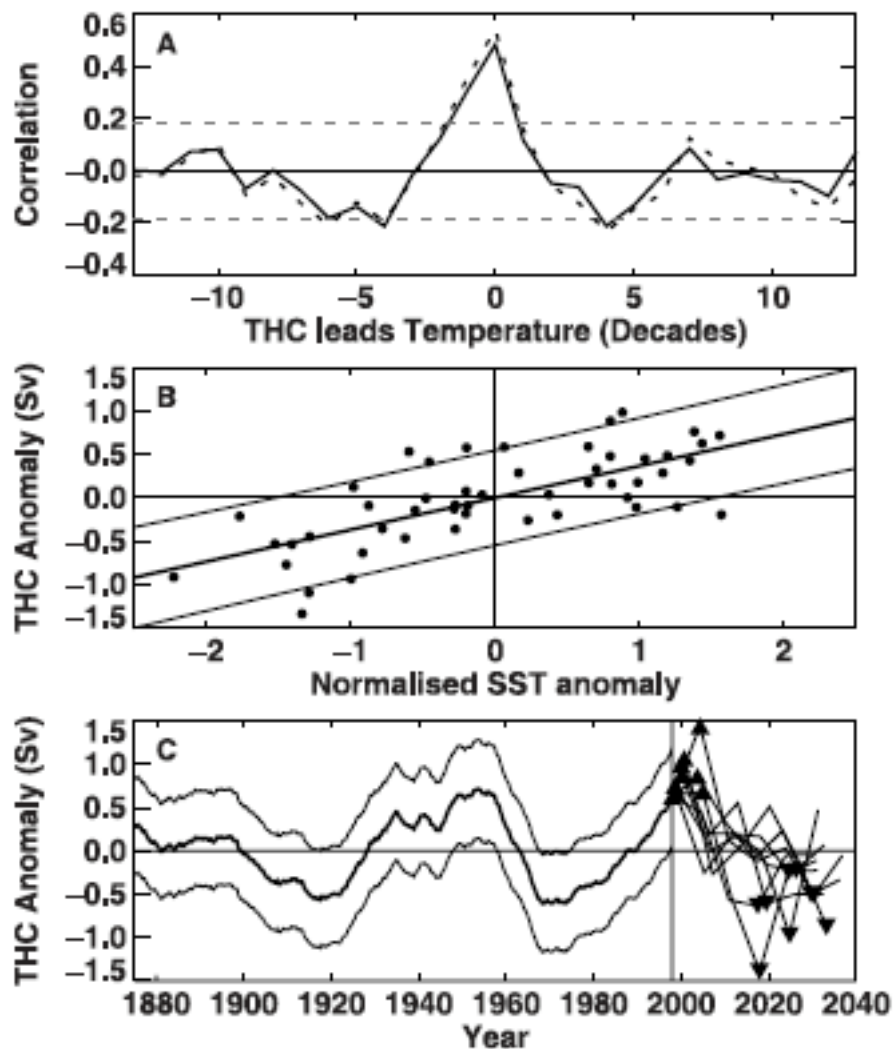


Figure 4. (a) Cross-correlations of decadal global (solid curve) and Northern Hemisphere (dotted) mean surface temperatures with the THC index for 1400 years of simulation. 95% confidence limits are shown as dotted horizontal lines. Negative values on the abscissa indicate temperature leading the THC. (b) Decadal THC anomalies (Sv) for the 50 decades used in Figure 3 as a function of a normalised index of mean northern North Atlantic SST anomaly (points). The index is an area-average (100 W–20 E, 35–80 N) weighted by the local signal to noise variance ratio to reduce the influence of noisy marginal areas. The least-squares fit (thick line) is also a good fit for the remaining 900 years. 85% confidence intervals of the residuals are shown by thin curves. (c) Reconstruction of the THC (thick curve) and its uncertainty limits (thin curves), inferred using the regression and residual limits in Figure 4b and quadratically detrended running decadal mean SSTs from HadISST. The observed SSTs are weighted, meaned and normalised as the model SSTs. Dates refer to decadal mid-points. Also shown are the 8 forecast segments corresponding to the model THC after rises through the reconstructed 1993–2002 value (0.63 Sv). Assuming an AMO period closer to the 65 years estimated from observations than the 100 years in the simulation, the segments are contracted so 6 decades of model THC produce a forecast for 35 years. Upward- and downward pointing triangles denote maxima and minima respectively of the THC ensemble members.

Mann & Emanuel, 2006

- Goldenberg et al., 2001
 1. define the AMO as a remnant after linearly detrending North Atlantic SST data from 1870 to 2000 (Linear + AMO)
 2. attribute the AMO as having a significant influence on tropical North Atlantic SST
- Mann and Park, 1994:
 1. Analyses using multivariate signal detection methods to separate possible long-term oscillatory patterns from trends in observational data
 2. AMO has lesser influence
- Knight et al., 2005:
 1. model simulations
 2. AMO has lesser influence

Mann & Emanuel, 2006

- Univariate
 - $T(t) = a_0 G(t) + R_0(t)$
 - T: 1870 to 2004 ASO HadISST2 of North Atlantic MDR
 - G: 1870 to 2004 Global Mean ASO SST
 - $a_0 = 0.93 \pm 0.12$; $sd(R_0) = 0.11$, but not robust
- Bivariate
 - $T(t) = aG(t) + bS(t) + R(t)$
 - S: Estimated NH anthro. aerosol forcing thru' 1999 (Crowley, 2000)
 - $a = 1.7 \pm 0.17$; $b = 0.79 \pm 0.16$
 - -0.50°C estimated regional enhancement of aerosol cooling!
- Assumes AMO does not project onto Global Mean SST
 - Knight, 2005 finds 0.05°C peak amp. AMO contribution to G which has increased by about 0.8°C

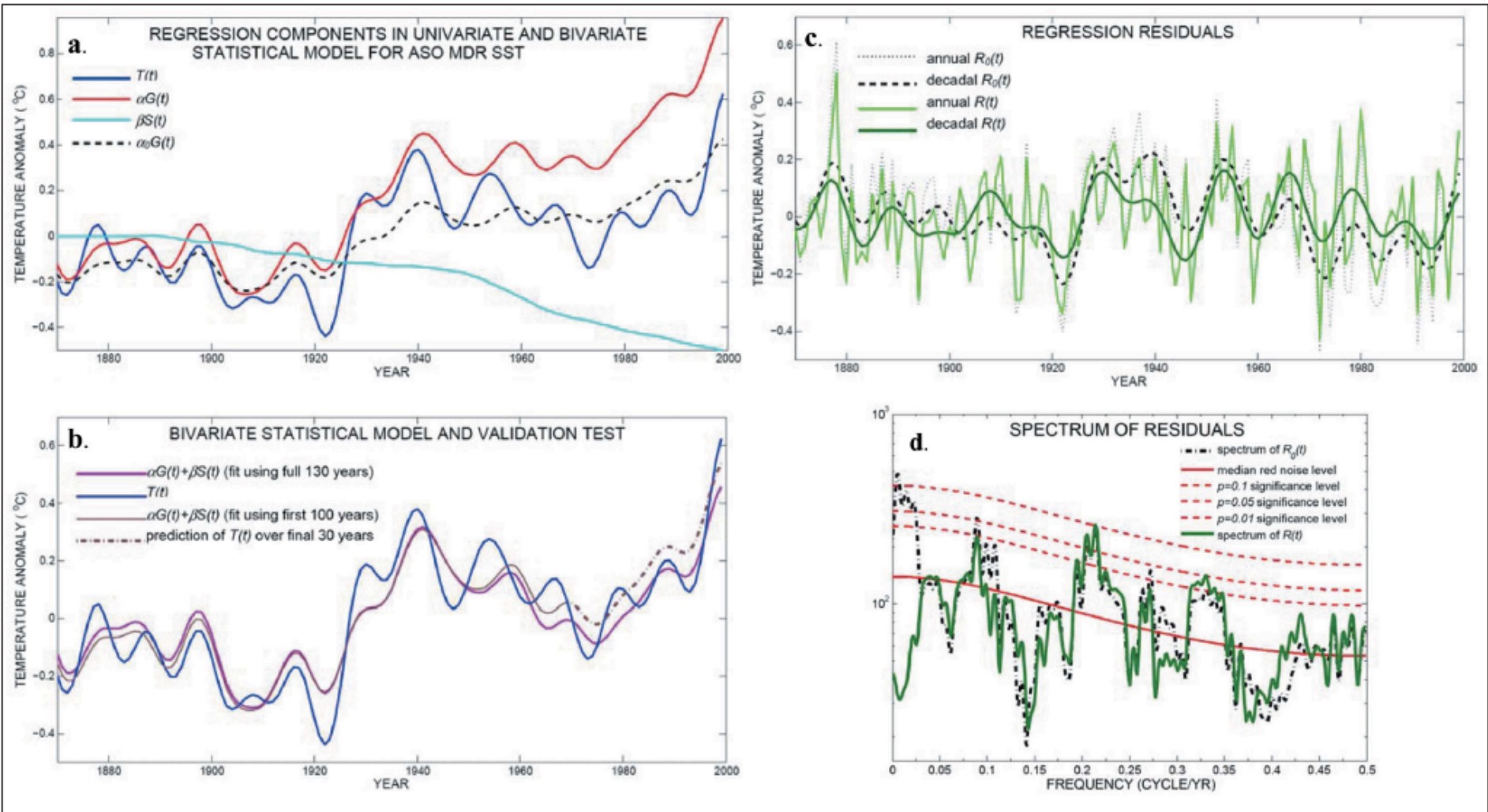


Fig. 1. Analyses of sea surface temperature (SST) series. (a) Decadally smoothed August-September-October (ASO) main development region (MDR) SST series $T(t)$ and estimated components for both (1) univariate regression [equation (1)] using ASO global mean SST [$\alpha G(t)$] and (2) bivariate regression [equation (2)] including the components associated with ASO global mean SST [$\alpha G(t)$] and the regional enhancement of anthropogenic tropospheric aerosol cooling [$\beta S(t)$]. (b) Bivariate statistical model [equation (2)] for $T(t)$ based on the sum of both regression components shown in Figure 1a. Shown also is the fit of the regression model based on the restricted interval 1870–1969 and the prediction of $T(t)$ over the subsequent 30 years (1970–1999) based on that regression model. (c) Annual and decadal smoothed univariate [$R_0(t)$] and bivariate [$R(t)$] regression residuals. (d) Power spectrum of univariate [$R_0(t)$] regression residuals, with estimated red noise level and associated $p = 0.1, 0.05,$ and 0.01 significance levels. Shown for comparison is the spectrum for the bivariate regression residual [$R(t)$]. See additional material for further details.

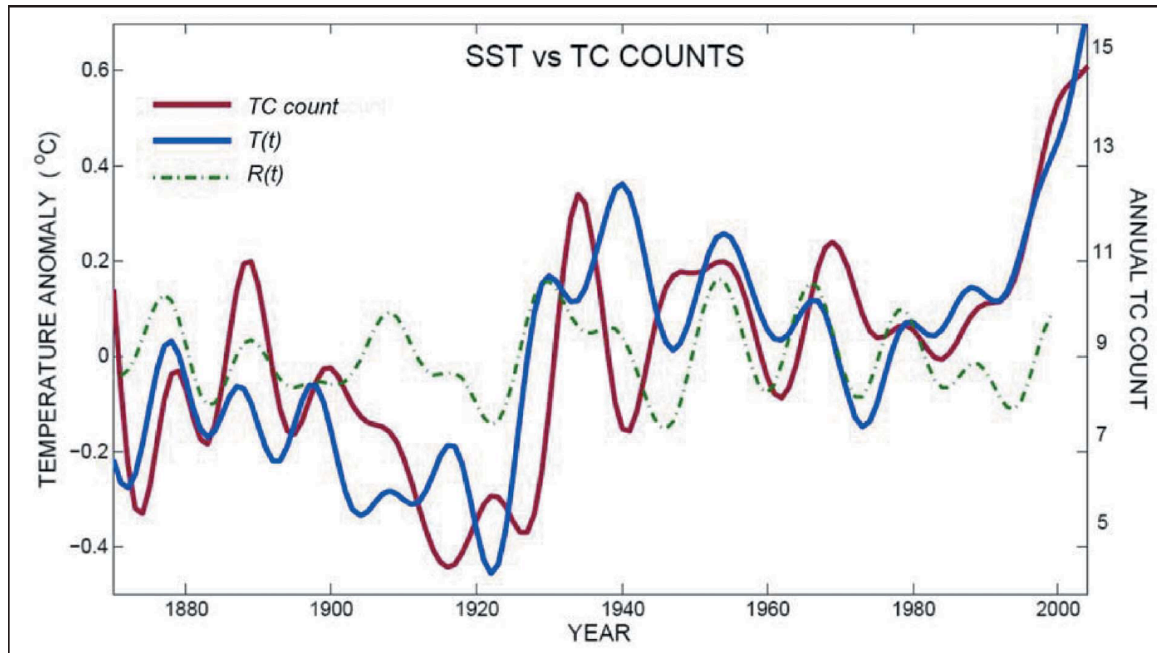


Fig. 2. Comparison of decadal smoothed tropical cyclone numbers with decadal smoothed ASO MDR SST series $T(t)$ and decadal smoothed bivariate regression residual series $R(t)$.

Note however, that TC count does not correlate with SST in the Pacific!

Summary of Mann & Emanuel, 2006

- Separate the influence of anthropogenic and natural factors rather than linear and oscillation
- Attribute long-term trend in tropical Atlantic SST and tropical cyclone activity to anthropogenic influences
- Implicate cooling effects of anthropogenic aerosols in tempering SST response to anthropogenic influences